CHAPTER 2 — TEMPERATURE

CHAPTER 2 — TEMPERATURE

2.1 Thermodynamics and the tephigram

In the tephigram straight-line rectangular co-ordinates are T (temperature) and ϕ (entropy); dry adiabats are, therefore, perpendicular to the isotherms. Equal area represents equal energy at any point, simplifying geopotential calculations.

2.1.1 Constructions using a tephigram

Fig. 2.1 illustrates Normand's theorem and construction to obtain potential and equivalent temperatures. **Fig. 2.2** illustrates constructions to obtain vapour pressure and saturation vapour pressure. Temperatures are specified for a parcel of air at 850 hPa.

HWF (1975)

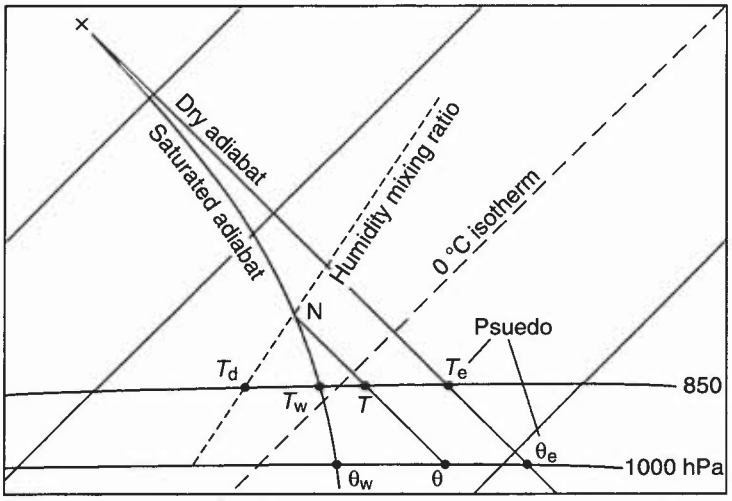

Figure 2.1. Construction on a tephigram to illustrate Normand's theorem, and to obtain potential temperature (θ, θ_w) and pseudo-equivalent temperatures (T_e, θ_e). The constructions are based on a parcel of air at 850 hPa, with temperature (T), wet-bulb temperature (T_w) and dew point (T_d).

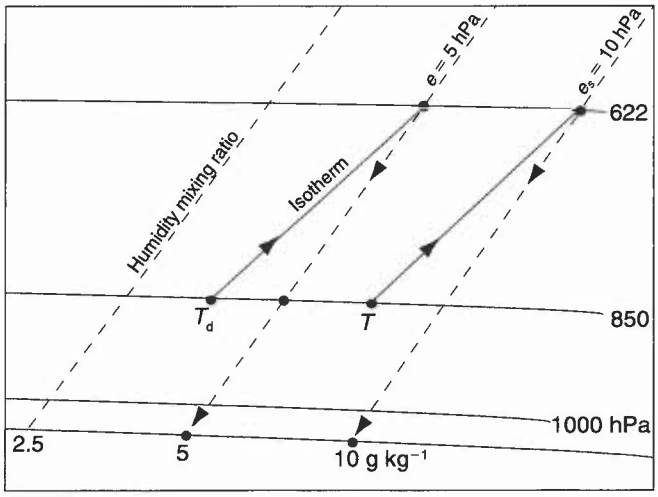

Figure 2.2. Constructions on a tephigram to obtain vapour pressure (e) and saturation vapour pressure (e_s) based on the air temperature (T) and dew point (T_d) of a parcel of air at 850 hPa.

2.1.2 Calculation of heights on a tephigram

This is illustrated in **Fig. 2.3**. After modifying the profile to show the virtual temperature (T_v):

(i) divide the temperature profile into a series of layers, 100 hPa deep up to the 300 hPa isobar, and then 50 hPa deep between 300 and 100 hPa.

(ii) Use a transparent scale marked with a straight line. Lay this over the temperature profile in each of the layers, parallel to the isotherms so as to create equal positive and negative areas either side of the mean isotherm.

(iii) Read off the layer thicknesses, in decametres, as marked along the intermediate isobars at 950, 850, 750 hPa, etc. The height of a standard pressure level is the sum of all the partial thicknesses below that level, plus the height of the 1000 hPa level. The height of the 1000 hPa surface may be read off from the nomogram printed on standard tephigrams. When the MSL pressure is less than 1000 hPa, the 1000 hPa heights are negative.

The formula for height calculations involving layers which are not at standard levels is:

$$H = 29.27\, T_v \ln(p_0/p_1)$$

where H is in metres and T_v is the mean virtual temperature (K) of the layer $p_0 - p_1$.

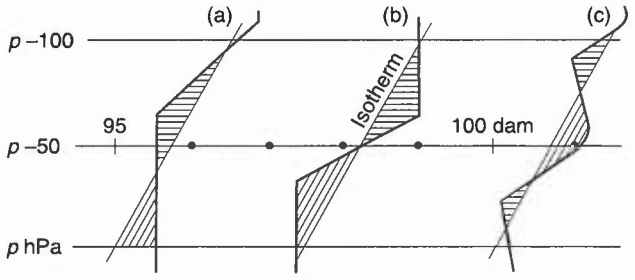

Figure 2.3. Calculating the thickness of a 100 hPa layer (base pressure = p). Shaded areas show equal positive and negative areas either side of a mean isotherm for three different shapes of environment curve. Thickness values are read off the scale on intermediate isobars. The examples show thickness values of (a) 95.7 dam, (b) 98.2 dam, and (c) 100.7 dam. See text for method of calculation.

2.2 Diurnal temperature variations in different air masses

(i) Statistics of temperature ranges occurring in various conditions can help in deciding whether forecast temperatures are reasonable.

(ii) In **Table 2.1** air-mass types are grouped according to whether trajectories on approaching the British Isles are curved cyclonically or anticyclonically. Data are pre-1950.

(iii) Forecasters may well have local data.

Table 2.1. Diurnal variation of temperature (°C) at Kew and Rye in different conditions

	Kew (1871–1940)					Rye (1945–1948)			Kew (1950–1954) Clear days		
Month	Polar (cyclonic)	Polar and tropical (anticyclonic)	Tropical (straight trajectory) maritime	Tropical (straight trajectory) continental	All occasions	All occasions	Clear days	Cloudy days	Average	Maximum	Minimum
Jan.	3.5	5	2	2	5	3	6	1	5	6.5	4.5
Feb.	4.5	5.5	3	5.5	5.5	3.5			7.5	8.5	7
Mar.	5	6.5	4.5	8.5	7	7			9.5	16.5	5.5
Apr.	6	8.5	4.5	10.5	8.5	8			11.5	18	7
May	7	9.5	8	11.5	9.5	8.5			12	16.5	8
June	7	9	6.5	10.5	9.5	7.5			12.5	17.5	8.5
July	6.5	9.5	6.5	11.5	9	8	13.5	3.5	11	14	8.5
Aug.	6.5	9.5	6.5	11.5	9	8.5			10.5	15	7.5
Sept.	6	8	6	9	8.5	7			10	15	7
Oct.	5.5	6.5	4	7	7	7			9.5	12	5
Nov.	4.5	5.5	2	5	5.5	4			7	11.5	4.5
Dec.	4	5	2	4	5	2.5			6	8	4

These data are summarized in the Local Weather Manual for S England, which also presents the 850 hPa WBPT by air-mass track and by season.

Belasco (1952)
Local Weather Manual (S England) (1994)

2.3 Daytime rise of surface temperature

2.3.1 Forecasting the hourly rise of temperature on sunny days, using a tephigram

This method relates the amount of solar energy available for heating the lower layers of the atmosphere to an equivalent area on a tephigram.

(i) **Table 2.2** gives the thickness of the layer (Δp in hPa) which is changed from an isothermal to an adiabatic state by insolation for each hour from dawn, to the time of day maximum temperature, for the middle of each month, assuming no cloud.

(ii) Marking isobars p_o (the QFE) and $p_o - \Delta p$ **(Fig. 2.4)**, point I is placed on the isobar ($p_0 - \Delta p$) with JIF along a dry adiabat and IH along an isotherm in such a way that it intersects the environment curve to form equal areas on either side, i.e. in this case area BAD equals area GHA plus area BIE. The point F then gives the value of the forecast surface temperature. This assumes no superadiabat at the surface (e.g. to F′). See note (i) below.

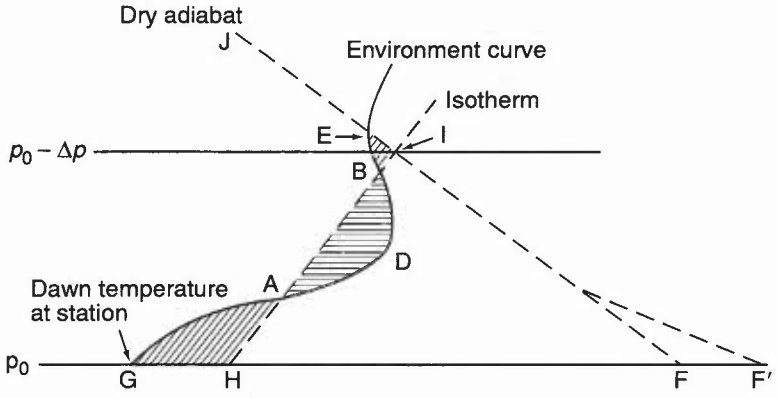

Figure 2.4. Estimating the rise of temperature on a sunny day by a tephigram construction. Δp is the thickness of the layer (hPa) and F is the forecast surface temperature. See text for details of construction.

Table 2.2 The thickness of the layer (Δp in hPa) which is changed from an isothermal to an adiabatic state by insolation at 52° N, 00° W

Month	Time (UTC)											
	05	06	07	08	09	10	11	12	13	14	15	Max
Jan.	—	—	—	—	03	18	35	48	58	61		61
Feb.	—	—	—	01	15	33	50	65	75	80		81
Mar.	—	—	02	17	35	53	68	81	90	95		97
Apr.	—	04	19	37	54	71	86	98	107	112	115	115
May	04	19	36	54	70	86	100	110	119	124	127	127
June	08	23	40	58	74	89	102	113	122	127	130	131
July	04	19	36	53	69	84	98	109	118	123	126	126
Aug.	—	08	24	41	59	75	89	101	110	116	119	119
Sept.	—	—	10	27	44	60	76	88	96	102	104	104
Oct.	—	—	01	13	29	45	60	72	80	85		86
Nov	—	—	—	—	11	25	38	49	57	61		61
Dec.	—	—	—	—	02	15	30	42	50	53		53

Notes:

(i) These values do not take into account any superadiabatic close to the surface. Add 2 °C (or more, according to local experience) to the resulting forecast temperature with clear skies and light winds in summer, to allow for superadiabats.

(ii) Approximate corrections to be applied to allow for cloud cover:

Table 2.3.

8/8 Ci	use	90% of depth (Δp in hPa)
8/8 As	use	60%
8/8 Sc	use	50%
8/8 Ns	use	35%

The value of Δp may be reduced if the ground is wet, covered in snow/hoar frost and/or the lowest layers of the atmosphere are very humid. In summer, if the ground is very dry and humidity in the bottom layers is low, the value of Δp may be increased. These changes are generally only significant in the first 3 or 4 hours of heating.

Inglis (1970)
Jefferson (1950)
Johnson (1958)

2.3.2 Forecasting the temperature rise on days with fog or low cloud (Jefferson's method)

(i) Use the method in 2.3.1 to draw a curve showing the rise of temperature to be expected if the sky were clear.

(ii) Evaluate a constant 'delay factor' f. This may be done from the observation of temperature at least 3 hours after sunrise (T_3). If h_0 is the time of sunrise, h_2 is the time at which the temperature is observed and h_1 is the time at which that temperature would have been observed on a sunny day, then

$$f = (h_1 - h_0)/(h_2 - h_0)$$

(iii) Plot points C, F, etc., as shown in **Fig. 2.5**, such that:

$$AB/AC = DE/DF = \ldots f.$$

(As a first estimate, take $f = 0.25$ for deep fog or thick stratus and $f = 0.35$ for shallow fog or thin stratus). Points C, F, etc. provide a forecast temperature curve for a foggy day.

(iv) If this curve reaches the temperature (T_c) at which the fog can be expected to disperse, the subsequent temperature rise will be steeper and more in line with conditions for a clear day (dotted line in **Fig. 2.5**).

(v) A note of caution: the local advection of fog will give large errors in T_c, the calculated value not being achieved.

Grant (undated)
Jefferson (1950)

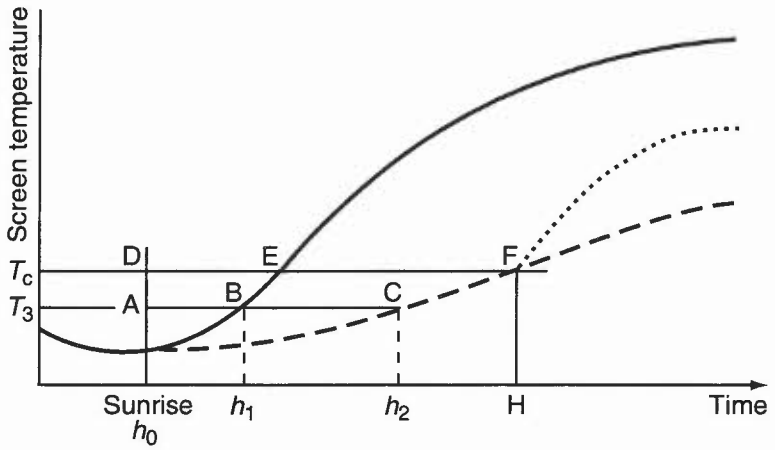

Figure 2.5. Constructing a forecast temperature curve on a foggy morning. The solid line is the forecast temperature curve for a clear day. The dashed line is the forecast for a foggy day, based on a delay factor of 0.35. The dotted line is the forecast for the later part of the day if the fog clears when the temperature reaches the critical value (T_c), at time H. See text for details of construction.

2.3.3 Forecasting T_{max} (Callen and Prescott's method, using 1000–850 hPa thickness)

This is an empirical method based on the maximum temperatures observed at Gatwick and the 1000–850 hPa thickness values at midday at Crawley.

There are three steps:

(i) Classify the cloud cover or presence of fog between dawn and 1200 UTC on a scale from 0 to 3 (**Table 2.4**), as follows:

Table 2.4.

Class 0	$C_L + C_M \leqslant 3/8$, $C_H \leqslant 5/8$; or any fog confined to dawn period.
Class 1	$C_L + C_M + C_H = 4/8$–$6/8$; or any fog clearing slowly during morning.
Class 2	$C_L + C_M \geqslant 6/8$; or any fog clearing before noon.
Class 3	Predominantly overcast with precipitation (not including very slight drizzle) or persistent fog.

(ii) Using **Fig. 2.6**, obtain the temperature adjustment for the month for the appropriate cloud class.
(iii) Apply this adjustment to the values given in **Table 2.5** to find the predicted maximum temperature.

The relationship between 1000–850 thickness (h) and the unadjusted maximum temperature (T_u) is given by

$$T_u = -192.65 + 0.156h.$$

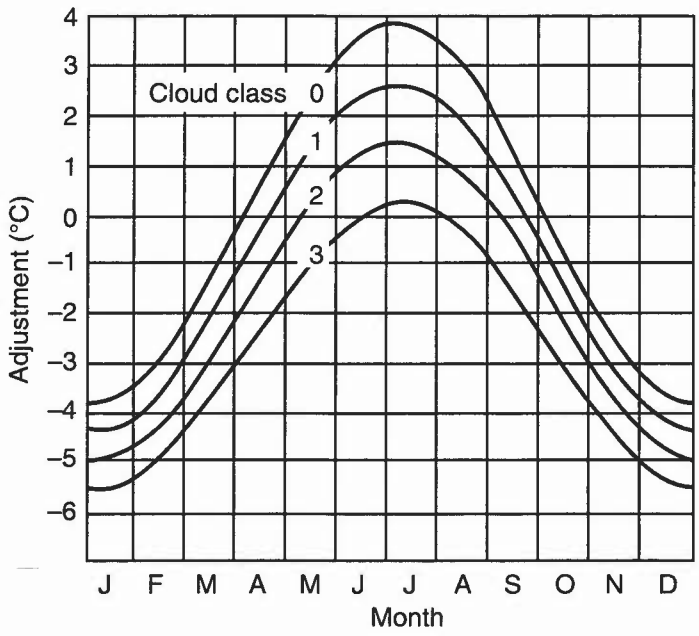

Figure 2.6. Adjustments to be applied to the values in Table 2.5 to allow for cloud classification and time of year.

Table 2.5. Unadjusted maximum temperature (°C) in terms of 1000–850 hPa thickness

Thickness (gpm)	Maximum temperature									
	0	1	2	3	4	5	6	7	8	9
1230	−0.8	−0.6	−0.5	−0.3	−0.1	0.0	0.2	0.3	0.5	0.6
1240	0.8	0.9	1.1	1.3	1.4	1.6	1.7	1.9	2.0	2.2
1250	2.3	2.5	2.7	2.8	3.0	3.1	3.3	3.4	3.6	3.8
1260	3.9	4.1	4.2	4.4	4.5	4.7	4.8	5.0	5.2	5.3
1270	5.5	5.6	5.8	5.9	6.1	6.2	6.4	6.6	6.7	6.9
1280	7.0	7.2	7.3	7.5	7.7	7.8	8.0	8.1	8.3	8.4
1290	8.6	8.7	8.9	9.1	9.2	9.4	9.5	9.7	9.8	10.0
1300	10.1	10.3	10.5	10.6	10.8	10.9	11.1	11.2	11.4	11.6
1310	11.7	11.9	12.0	12.2	12.3	12.5	12.6	12.8	13.0	13.1
1320	13.3	13.4	13.6	13.7	13.9	14.0	14.2	14.4	14.5	14.7
1330	14.8	15.0	15.1	15.3	15.5	15.6	15.8	15.9	16.1	16.2
1340	16.4	16.5	16.7	16.9	17.0	17.2	17.3	17.5	17.6	17.8
1350	17.9	18.1	18.3	18.4	18.6	18.7	18.9	19.0	19.2	19.4
1360	19.5	19.7	19.8	20.0	20.1	20.3	20.4	20.6	20.8	20.9
1370	21.1	21.2	21.4	21.5	21.7	21.8	22.0	22.2	22.3	22.5
1380	22.6	22.8	22.9	23.1	23.3	23.4	23.6	23.7	23.9	24.0
1390	24.2	24.3	24.5	24.7	24.8	25.0	25.1	25.3	25.4	25.6
1400	25.7	25.9	26.1	26.2	26.4	26.5	26.7	26.8	27.0	27.2
1410	27.3	27.5	27.6	27.8	27.9	28.1	28.2	28.4	28.6	28.7
1420	28.9	29.0	29.2	29.3	29.5	29.6	29.8	30.0	30.1	30.3
1430	30.4	30.6	30.7	30.9	31.1	31.2	31.4	31.5	31.7	31.8
1440	32.0	32.1	32.3	32.5	32.6	32.8	32.9	33.1	33.2	33.4

Callen et al. (1982)

2.3.4 Forecasting T_{max} from the 850 hPa wet-bulb potential temperature

The maximum temperature derived from the 850 WBPT is presented in **Table 2.6**, with corrections for wet and sunny conditions (based on London Weather Centre data for southern England).

Table 2.6. Maximum temperatures derived from 850 hPa wet-bulb potential temperatures

850 hPa θ_w	Equivalent thickness (m) 1000–850 hPa	Jan.	Feb.	Mar.	Apr.	May	Jun.	Jul.	Aug.	Sept.	Oct.	Nov.	Dec.	Correction Wet	Correction Sunny
18	1390	19	20	21	23	25	26	26	25	24	22	20	19	−5	+3
16	1380	17	19	19	21	23	25	25	23	23	21	19	17	−5	+2
14	1370	16	17	18	20	22	23	23	22	21	19	17	16	−4	+2
12	1360	15	15	17	19	21	21	21	21	19	17	15	17	−4	+2
10	1350	13	14	15	17	19	20	20	19	18	16	14	13	−4	+2
8	1340	11	13	13	15	17	19	19	17	17	15	13	11	−3	+2
6	1325	9	10	11	13	15	16	16	15	14	12	10	9	−3	+1
4	1320	8	9	10	12	14	15	15	14	13	11	9	8	−3	+1
2	1305	6	7	8	10	12	13	13	12	11	9	7	6	−3	+1
0	1295	4	5	6	8	10	11	11	10	9	7	5	4	−2	+1
−2	1285	3	4	5	7	9	10	10	9	8	6	4	3	−2	+1
−4	1270	−1	1	1	4	6	7	7	6	5	3	1	1	−2	+1

2.4 Nocturnal fall of surface temperature

(i) A number of techniques have been developed, based on empirical methods, to estimate the night minimum temperature during a clear night.

(ii) These depend on solving an equation of the form: $T_{min} = aT + bT_d + C$, where T is an afternoon temperature, T_d is the dew point at a particular time or a mean dew point over a cooling period and C is a quantity depending only on wind speed and cloud amount. a and b are constants.

(iii) Various methods for estimating T_{min} are presented, each using different ways of determining the constants a, b, and C. A useful approach is to estimate the dusk temperature as one of the points on the Saunders' cooling curve.

(iv) The methods are applicable only when the ground is not snow covered; the effect of fresh snow cover is discussed later. Exceptionally low minima may also occur when there is a large catchment area for katabatic drainage and when the lowest layers (950–850 hPa) are very dry (dew-point depressions >20 °C).

Boyden (1937) **McKenzie (1944)**

2.4.1 Forecasting dusk temperature, T_R, by Saunders' method

Saunders based his graphical method for determining a cooling curve on the idea of a discontinuity occurring in the rate of cooling at grass level within an hour after sunset, an effect particularly well defined on clear, windless nights (and possibly related to the deposition of dew).

He obtained regression equations relating the maximum temperature, T_{max}, and corresponding dew point, T_d, to T_R:

$$T_R = 0.5\,(T_{max} + T_d) - C$$

and C = 0.3 °C when no inversion with base below 900hPa
C = 2.2 °C when there is an inversion base below 900hPa.

Consider whether observed T_{max} and T_d will be representative of air mass expected over the site during the night.

Saunders established the approximate times for T_R (at Northolt) to be:

Table 2.7.

	Jan.	Feb.	Mar.	Apr.	May	June	July	Aug	Sept.	Oct.	Nov.	Dec.
UTC	1645	1800	1930	2045	2100	2115	2115	2045	1930	1745	1700	1630

If topsoil is wet T_R occurs about 1 hour earlier in late spring and early summer, and about ½ hour earlier in late summer.

Barthram refined this T_R technique to produce night-cooling nomograms for summer and winter, allowing for the effect of the geostrophic wind and cloud cover.

Barthram (1964) **Saunders (1952)**

2.4.2 Forecasting minimum temperature

2.4.2.1 Forecasting T_{min} (McKenzie's method)

(i) The night-time minimum air temperature (T_{min}) can be forecast as follows:

$$T_{min} = 0.5(T_{max} + T_d) - K$$

where T_{max} = maximum temperature, T_d = air-mass dew point at time of T_{max}, and K = local constant depending on forecast surface wind and low cloud amount).

(ii) Although originally for Dyce (Aberdeen) many inland low-level airports have values similar to those for Birmingham (**Table 2.8(a)**). Kensett has published K values for 90 UK stations.

Table 2.8(a). Values of local constant (K) for Birmingham Airport

Mean overnight surface wind (kn)	Average cloud amount overnight (oktas) 0	1–2	3–4	5–6	7–8
Calm	8.8	8.0	7.3	6.7	3.2
1–3	8.2	7.7	6.7	5.1	2.8
4–6	6.5	5.8	5.2	4.0	2.3
7–10	4.7	4.3	3.9	3.1	1.8
11–16	2.3	2.8	2.5	2.1	1.4
17–21	0.5	0.8	2.0	1.1	0.8

Monthly variations have been found which apply at all stations. The value of K may usefully be corrected by the following amounts:

Table 2.8(b).

	Jan.	Feb.	Mar.	Apr.	May	June	July	Aug.	Sept.	Oct.	Nov.	Dec.
A	−1.0	−0.5	+0.5	0.0	0.0	0.0	0.0	0.0	+0.5	+1.0	0.0	−1.0
B	−0.5	−0.5	0.0	0.0	+0.5	+0.5	+0.5	+0.5	0.0	0.0	−0.5	−0.5

A = 'Good radiation nights' B = 'Poor radiation nights'

Kensett (1983) **McKenzie (1944)**

2.4.2.2 Forecasting T_{min} (Craddock and Pritchard's method)

(i) The following regression equation was obtained from a statistical investigation of 16 stations in eastern England not close to the sea; it is considered valid for a wide area of eastern England:

$$T_{min} = 0.316\,T_{12} + 0.548\,T_{d12} - 1.24 + K$$
$$= X + K$$

where T_{12} = screen temperature at 1200 UTC and T_{d12} = dew-point temperature at 1200 UTC.

(ii) For ease of use, the value for X may be obtained from **Table 2.9** while the values for K, which depend on forecast values of the mean geostrophic wind and mean cloud amount, are given in **Table 2.10.** The means are forecast values for 1800, 0000 and 0600 UTC.

Table 2.9. Computation of the value of X (°C)

Air temp. at 1200	Dew-point at 1200 UTC −3	−2	−1	0	1	2	3	4	5	6	7	8	9	10	11	12	13	14	15	16
27	5.7	6.2	6.7	7.3	7.8	8.4	8.9	9.5	10.0	10.6	11.1	11.7	12.2	12.8	13.3	13.9	14.4	15.0	15.5	16.1
26	5.4	5.9	6.4	7.0	7.5	8.1	8.6	9.2	9.7	10.3	10.8	11.4	11.9	12.5	13.0	13.6	14.1	14.6	15.2	15.7
25	5.1	5.6	6.1	6.7	7.2	7.8	8.3	8.9	9.4	9.9	10.5	11.0	11.6	12.1	12.7	13.2	13.8	14.3	14.9	15.4
24	4.8	5.2	5.8	6.3	6.9	7.4	8.0	8.5	9.1	9.6	10.2	10.7	11.3	11.8	12.4	12.9	13.5	14.0	14.6	15.1
23	4.5	4.9	5.5	6.0	6.6	7.1	7.7	8.2	8.8	9.3	9.9	10.4	11.0	11.5	12.1	12.6	13.2	13.7	14.2	14.8
22	4.1	4.6	5.2	5.7	6.3	6.8	7.4	7.9	8.5	9.0	9.5	10.1	10.6	11.2	11.7	12.3	12.8	13.4	13.9	14.5
21	3.8	4.3	4.8	5.4	5.9	6.5	7.0	7.6	8.1	8.7	9.2	9.8	10.3	10.9	11.4	12.0	12.5	13.1	13.6	14.2
20	3.5	4.0	4.5	5.1	5.6	6.2	6.7	7.3	7.8	8.4	8.9	9.5	10.0	10.6	11.1	11.7	12.2	12.8	13.3	13.8
19	3.2	3.7	4.2	4.8	5.3	5.9	6.4	7.0	7.5	8.1	8.6	9.1	9.7	10.2	10.8	11.3	11.9	12.4	13.0	13.5
18	2.9	3.4	3.9	4.4	5.0	5.5	6.1	6.6	7.2	7.7	8.2	8.8	9.4	9.9	10.5	11.0	11.6	12.1	12.7	13.3
17	2.6	3.0	3.6	4.1	4.7	5.2	5.8	6.3	6.9	7.4	8.0	8.5	9.1	9.6	10.2	10.7	11.3	11.8	12.4	12.9
16	2.3	2.7	3.3	3.8	4.4	4.9	5.5	6.0	6.6	7.1	7.7	8.2	8.7	9.3	9.8	10.4	10.9	11.5	12.0	12.6
15	1.9	2.4	3.0	3.5	4.0	4.6	5.1	5.7	6.2	6.8	7.3	7.9	8.4	9.0	9.5	10.1	10.6	11.2	11.7	
14	1.6	2.1	2.6	3.2	3.7	4.3	4.8	5.4	5.9	6.5	7.0	7.6	8.1	8.7	9.2	9.8	10.3	10.9		
13	1.3	1.8	2.3	2.9	3.4	4.0	4.5	5.1	5.6	6.2	6.7	7.3	7.8	8.3	8.9	9.4	10.0			
12	1.0	1.5	2.0	2.6	3.1	3.6	4.2	4.7	5.3	5.8	6.4	6.9	7.5	8.0	8.6	9.1				
11	+0.7	1.1	1.7	2.2	2.8	3.3	3.9	4.4	5.0	5.5	6.1	6.6	7.2	7.7	8.3					
10	+0.4	+0.8	1.4	1.9	2.5	3.0	3.6	4.1	4.7	5.2	5.8	6.3	6.9	7.4						
9	−0.0	+0.5	1.1	1.6	2.2	2.7	3.2	3.8	4.3	4.9	5.4	6.0	6.5							
8	−0.4	+0.2	+0.7	1.3	1.8	2.4	2.9	3.5	4.0	4.6	5.1	5.7								
7	−0.7	−0.1	+0.4	1.0	1.5	2.1	2.6	3.2	3.7	4.3	4.8									
6	−1.0	−0.4	+0.1	+0.7	1.2	1.8	2.3	2.8	3.4											
5	−1.3	−0.8	−0.2	+0.3	+0.9	1.4	2.0	2.5	3.1											
4	−1.6	−1.1	−0.5	+0.0	+0.6	1.1	1.7	2.2												
3	−1.9	−1.4	−0.8	−0.3	+0.3	+0.8	1.4													

Table 2.10. Values of K (°C) based on mean forecast values of wind speed and cloud amount for 1800, 0000 and 0600 UTC

Mean geostrophic wind speed (kn)	Mean cloud amount (oktas) 0–2	2–4	4–6	6–8
0–12	−2.2	−1.7	−0.6	0
13–25	−1.1	0	+0.6	+1.1
26–38	−0.6	0	+0.6	+1.1
39–51	+1.1	+1.7	+2.8	—

The development of appropriate regression equations is required if the method is to be applied to other areas of the country.

Craddock et al. (1951)

2.4.2.3 Forecasting the hourly fall of temperature during the night (Barthram's method)

The following steps are used in conjunction with the Night Cooling Nomogram (**Fig. 2.7**), to obtain a cooling curve, drawn realistically through T_{max}, T_R (the Saunders' discontinuity temperature) and T_{min}:

(i) Use a representative upper-air sounding to determine whether there is an inversion with its base below 900 hPa at the time of maximum temperature.
(ii) Decide if nocturnal cloud cover will be best described as cloudless or 8/8.
(iii) From steps (i) and (ii), select one of the four rows marked 'Dew-point at time of maximum temp'. A series of vertical lines descends from these dew-point values.
(iv) Follow a horizontal line from the value for the maximum temperature (marked on the left-hand side) until it cuts the vertical line descending from the dew-point value selected in step (iii). From this point, follow one of the diagonal lines to the line marked 'Saunders' discontinuity temperature T_R'. Ignore T_R on cloudy, windy nights.
(v) The time of this discontinuity depends on the date. Use the small graph at the bottom of the nomogram where the months are marked. Find the time of T_R for the required date from the curve marked 'time of discontinuity'.
(vi) Follow the vertical line upwards from the time of T_R and extend it to the main graph to meet the value of T_R established in step (iv).
(vii) The next stage brings in a correction for the forecast gradient wind overnight. Select one of the diagonal lines on the right-hand side of the nomogram marked 'gradient wind speed'.
(viii) Follow the horizontal line from T_R until it cuts the selected diagonal line marked 'gradient wind speed'. From this point of intersection, descend along a vertical line to the diagonal marked 'Minimum temp. under clear skies'. The preliminary value for T_{min} can be read off here.
(ix) The preliminary value for T_{min} needs corrections for cloud amount and wind speed. The two small graphs (lower left) show amounts to be added to the preliminary T_{min} value to allow for the effect of nocturnal cloud cover and wind.
(x) In summer a further correction is needed because the short nights give a reduced period for cooling. Use the small graph (lower right, **Fig. 2.7(b)**) to find this value.
(xi) After raising the preliminary T_{min} by adding the corrections in steps (ix) and (x) the final value of T_{min} is plotted on the main graph above the time for sunrise shown on the lower graph.
(xii) This fixes three points on the cooling curve: T_{max} at approximately mid afternoon, T_R and T_{min}. The cooling curve can be drawn through these three points.

There are small differences between cooling for summer and winter and separate diagrams are provided for winter (October to March) (**Fig. 2.7(a)**) and for summer (April to September) (**Fig. 2.7(b)**).

Notes:
(a) The method applies to nights without fog.
(b) Effect of snow cover is discussed next.

Barthram (1964)

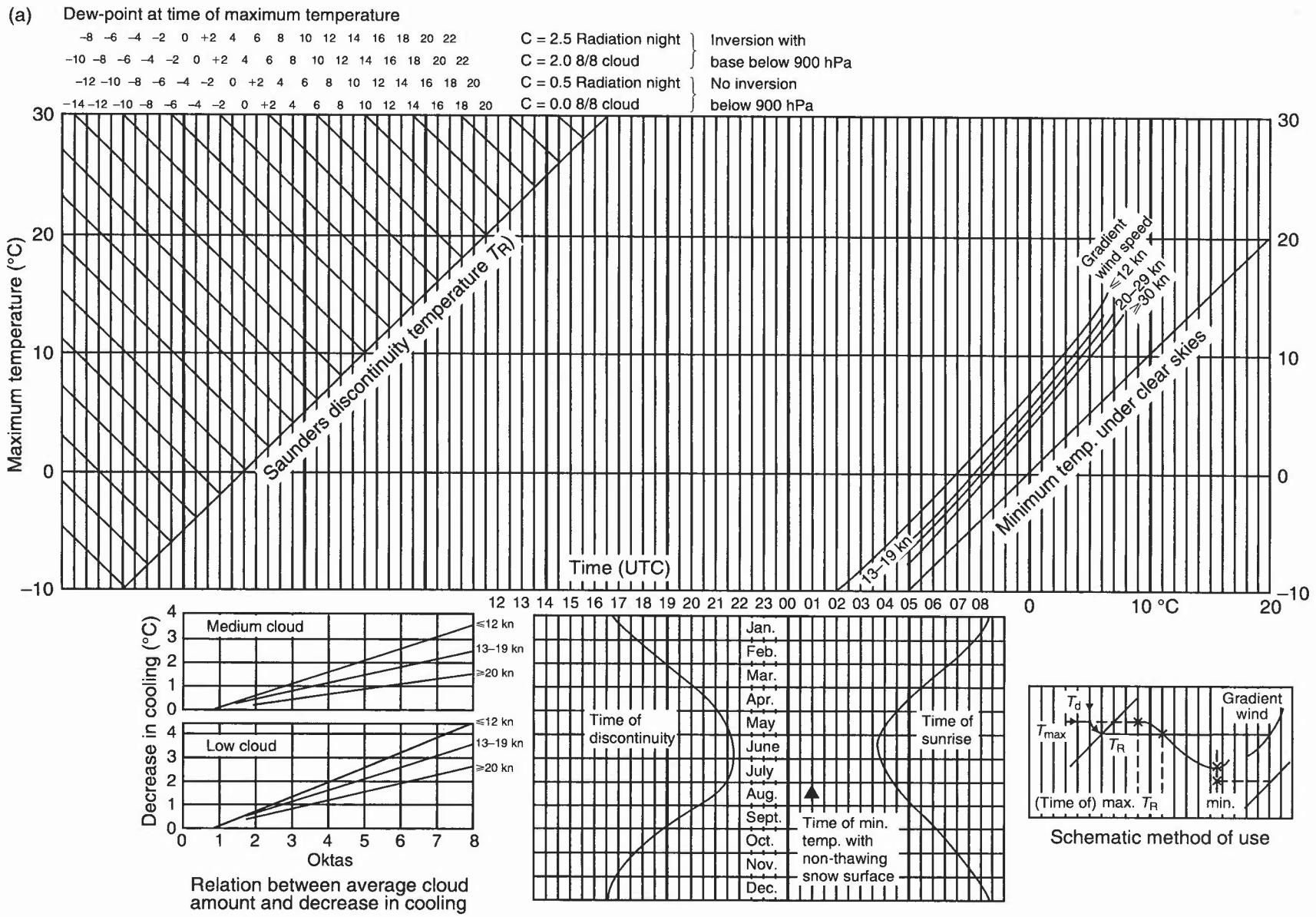

Figure 2.7(a). Night cooling nomogram for winter (October–March). See text for method of use.

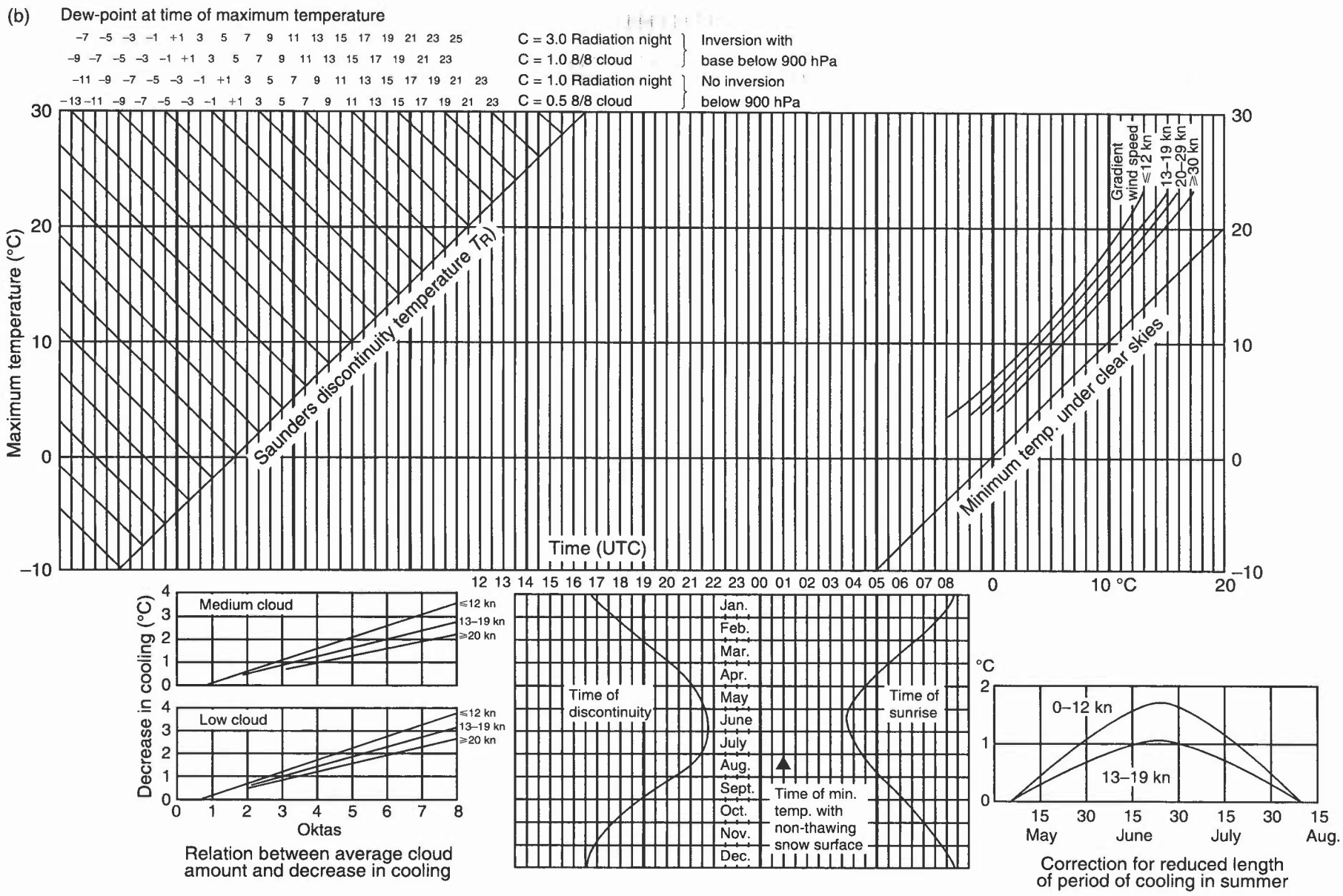

Figure 2.7(b). Night cooling nomogram for summer (April–September). See text for method of use.

2.4.3 *Effect of snow cover*

(i) Under clear skies and light winds, screen temperature over a snow surface is likely to fall 2 to 4 °C below the minimum calculated by the methods in 2.4 and to be reached earlier than if snow free.

(ii) With cloud present the minimum is likely to be about 1 °C lower than over snow-free surface; it may be less than that for wind speeds of 15 kn or so.

HWF (1975), Chapter 17.7.4

2.4.4 *Description of the severity of air frost*

When actual or forecast air temperatures fall below 0 °C, the severity of the frost is described arbitrarily by the terms 'Slight', 'Moderate', 'Severe' or 'Very severe' according to the temperature and the surface wind speed at the time, as illustrated in **Fig. 2.8.**

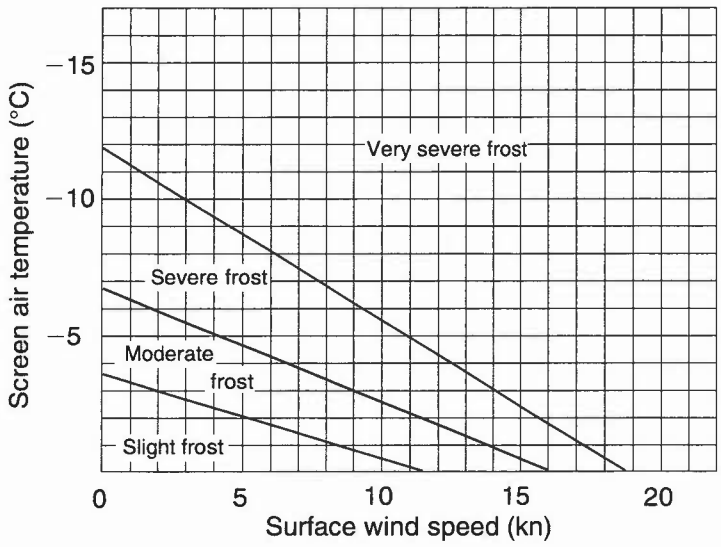

Figure 2.8. Diagram for determining the severity of air frost for actual or forecast wind speeds and air temperatures.

2.5 Grass- and concrete-minimum temperatures

2.5.1 *Forecasting the grass-minimum temperature, using the geostrophic wind speed and cloud amount*

T_g, the grass-minimum temperature is calculated from:

$$T_g = T_n - K$$

where T_n is the air-minimum temperature, and K is a constant which depends on forecast values of geostrophic wind speed and cloud amount.

Table 2.11. Values of K (°C)

V_g	N (oktas)			
(kn)	0–2	2–4	4–6	6–8
0–12	5.0	5.0	4.0	4.0
13–25	4.0	4.0	3.0	2.0
26–38	3.5	3.0	2.5	2.5
39–52	2.5	2.5	2.5	3.0

Values of V_g and N are means of the 1800, 0000 and 0600 UTC values.

Craddock & Pritchard (1951)
HWF (1975), Chapter 14.7.3

2.5.2 *Forecasting the grass-minimum temperature from the geostrophic wind speed (graphical method)*

Fig. 2.9 shows isopleths of the depression of the grass-minimum temperature below the air-minimum temperature at Cottesmore in eastern England. Only low-cloud cover is considered, and 'sky obscured' is taken to be the same as 8 oktas.

Sills (1969)

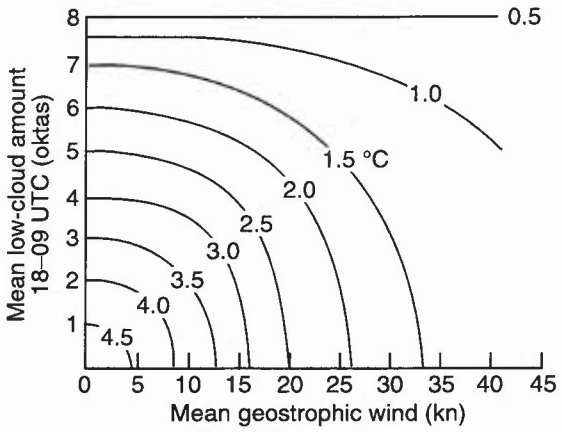

Figure 2.9. Depression (°C) of the grass-minimum temperature below the air-minimum temperature at Cottesmore.

2.5.3 *Forecasting the grass-minimum temperature from the surface wind speed*

Use the same formula as in 2.5.1 above but with values of K as follows:

Table 2.12. K values (°C) as a function of surface wind speed and cloudiness

Surface wind (kn)	Clear sky (up to 2/8)		Cloudy (8/8 cloud)
	Mean	(Max)	Mean
1–5	5.0	(8.0)	1.0
6–10	3.5	(8.6)	1.0
11–15	2.5	(3.5)	1.0
>15	1.5	(2.8)	1.0

Cloud cover is C_L, C_M or $C_L + C_M$

The mean values, averaged for six stations in England, have been rounded to 0.5 °C.

FRB (1993)

2.5.4 *Minimum temperature on roads*

At Watnall (near Nottingham), it was found that the difference between screen minimum, T_{min}, and (concrete) road minimum temperatures varied with the length of night. The following regression equation was obtained **(Table 2.13)**:

$$T_{min} - T_r = 0.28t - 2.9$$

where T_r = minimum temperature on the road, t is the length of night (in hours).

Table 2.13. Minimum temperature on roads (°C)

	Jan.	Feb.	Mar.	Apr.	May	June	July	Aug.	Sept.	Oct.	Nov.	Dec.
$T_{min} - T_r$ (observed)	2.0	1.5	1.0	0.0	—	—	—	—	—	0.5	1.5	2.0
From the formula for length of night for 52° N	1.5	1.1	0.5	0.0	−0.6	−1.1	−0.7	−0.3	0.3	0.8	1.4	1.6

Parrey (1969)
Ritchie (1969)

2.6 Forecasting road surface conditions

Forecasting the temperature of road surfaces is especially important in winter when icy conditions may occur. It is not straightforward, because of the wide variations in meteorological conditions which are found over short distances on the same night as well as variations in the thermal capacity and conductivity of different types of road and the road state (wet, ice-covered, salted, dry). Evaporation from the surface into dry ambient air will cool the surface.

2.6.1 Site differences

Site-specific ice prediction lies at the core of forecasting road surface conditions. There are three types of night for which forecasts are required: *Extreme, Damped and Intermediate.* **Fig 2.10** (for high and low sites).

2.6.1.1 Urban, rural and coastal sites and bridges

The following factors are important:

(a) *Urban and rural*
  (i) urban heat island (2.11) will give warmer air temperatures overnight;
  (ii) increased traffic flows cause increased turbulence; to simulate this forecast winds should be stronger in cities by 5 kn — even 10 kn on extreme radiation nights;

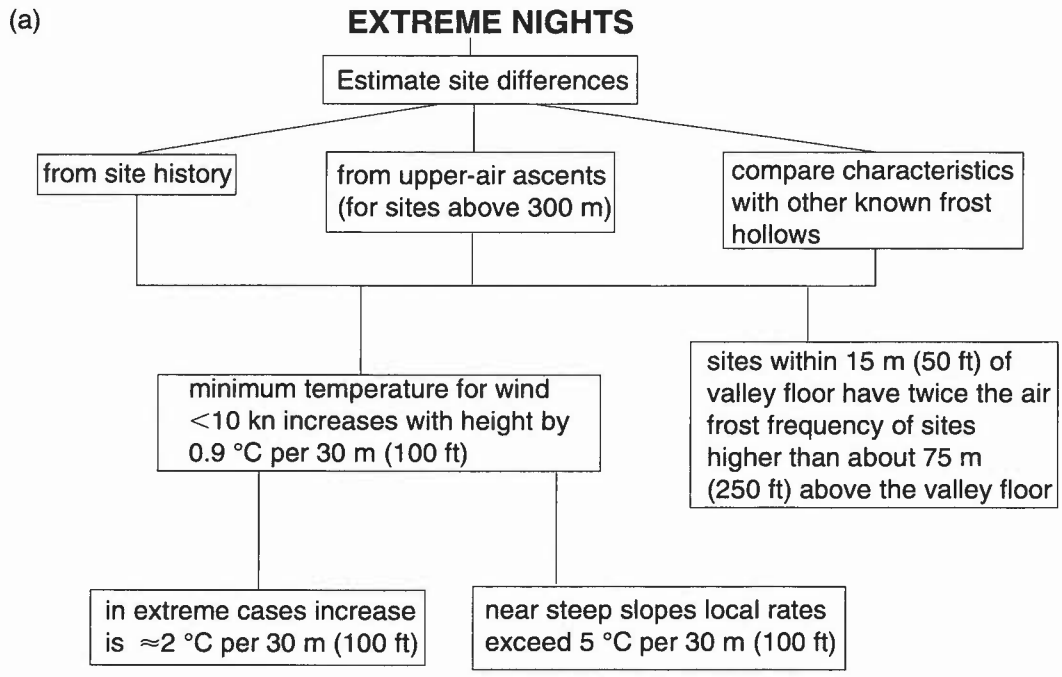

Figure 2.10. Forecasting road surface conditions — site differences. Select 'type of night'. EXTREME: clear, calm; generally katabatic drainage will ensure lowland sites colder than more elevated sites. Refer to Fig. 2.10(a). DAMPED: overcast, windy; giving well-mixed boundary layer. Refer to Fig. 2.10(b). INTERMEDIATE: wind/no cloud or cloud/no wind or rapidly changing conditions. Refer to Fig. 2.10(c). Note: high-level valleys will be subject to katabatic drainage from higher sites and show frost-hollow characteristics. Since these sites may be colder than lower sites due to altitude, they are often the coldest type of site, especially if sheltered. If not sheltered this will be similar to other high-altitude sites. Site history will be a useful indicator.

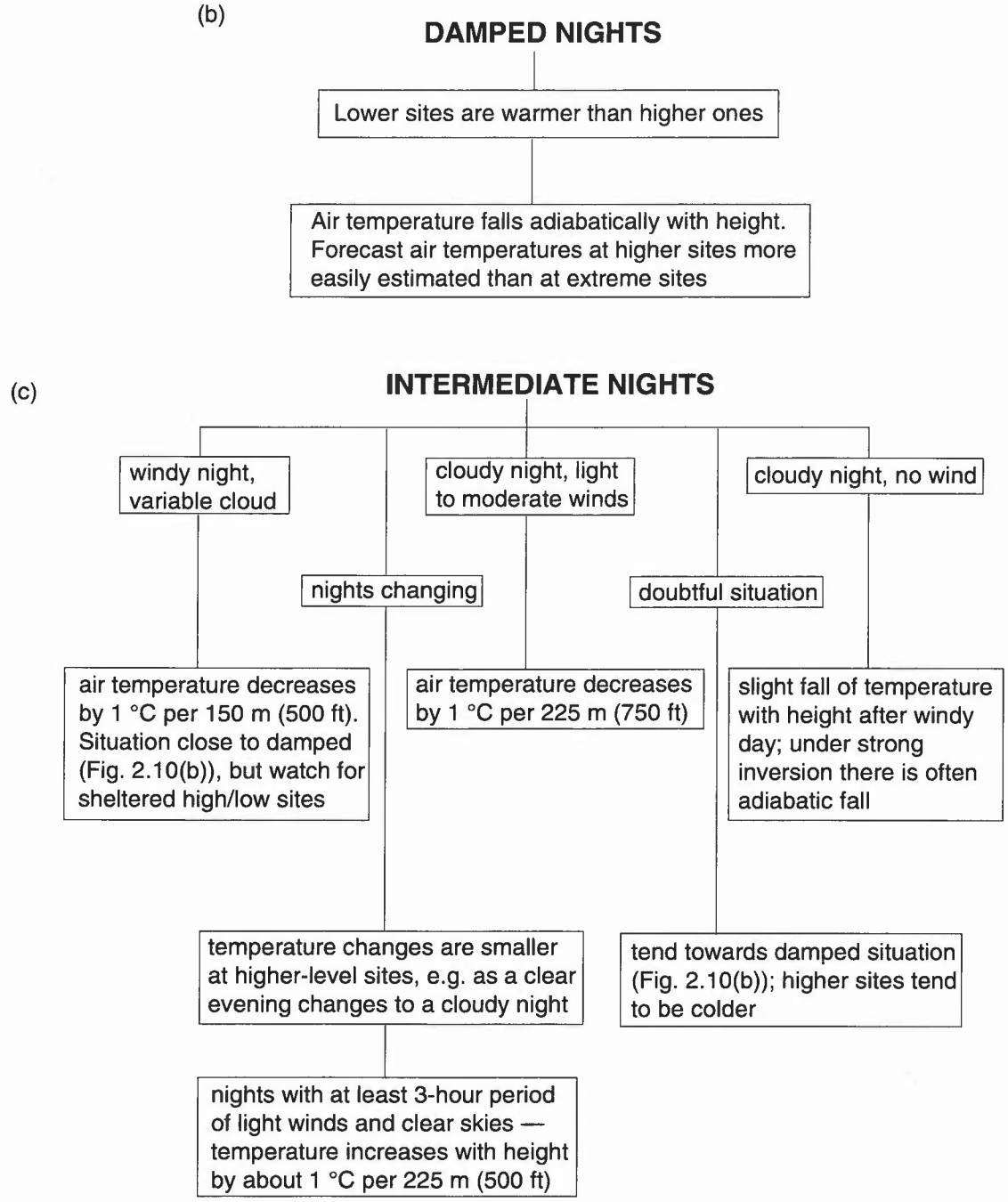

Figure 2.10. (Continued).

(iii) heavier traffic flows and buildings impede outgoing long-wave radiation; forecast clouds should be increased by 2 oktas to compensate (more for exceptional traffic flows);

(iv) well exposed *rural* sites will be the standard, requiring little adjustment although busy rural roads (e.g. motorways) may need adjustment which will be indicated by site history; these adjustments may need toning down to allow for the 'Sunday Effect'.

(b) *Coastal sites*

(i) can be warmer than inland sites when the wind comes off the sea;

(ii) sandy soils can point to a rapid drop of temperature on favoured nights;

(iii) greater dew points and greater likelihood of daytime showers favour widespread icing compared with inland;

(iv) site history is important;

(v) the forecasting aim is to determine the overnight wind direction.

(c) *Bridge decks*
   (i) have no ground heat flux, a small heat capacity;
   (ii) road surface temperatures (RST) will respond quickly to external forcing factors;
   (iii) the difference between bridges and roads will be greatest at times of greatest soil heat fluxes (especially late October/early November);
   (iv) location factor is dominant (e.g. estuarine, elevated urban).

Astbury (1994)
Perry & Symons (1991)

2.6.2 Forecasting for icy roads

Sources of moisture leading to road icing: precipitation; dew; hoar frost; freezing fog; moisture advection; melting snow; seepage; other sources (springs etc.).

(a) *Precipitation*
   (i) Widespread ice only forms twice in an average southern England winter.
   (ii) The central crown of the road will dry quickly after rain; ice will not become widespread, but will form in prone locations.
   (iii) Road temperatures need to fall below freezing within 2 hours of the cessation of rainfall for widespread ice.
   (iv) Late, prolonged showers from a trough followed by clear skies and light winds in the early evening can present a dangerous combination; salt may be washed off by later showers, with possible freezing following.
   (v) Forecasters must be aware of the necessity to update local authorities.
   (vi) Particular scenarios to note:
   rapid frontal clearance —
   heavy precipitation associated with a slow moving ana-front may be followed by rapid clearance and light winds;
   low road temperatures during precipitation —
   if rain turns to sleet or wet snow before clearing or under wintry showers, the latent heat to melt ice/snow will cool the road; a rapid drop of surface temperature below zero may result if skies then clear (even if a breeze persists or the cloud break is not continuous).

(b) *Freezing rain/drizzle*
   (i) The type of ascent involved is, typically, when a warm front approaches a surface intensely cooled due to radiation or by low-level cold advection.
   (ii) It is possible to get freezing drizzle from a complete sub-zero ascent. If no ice particles are present in the stratiform cloud (likely if temperatures are just below zero), then coalescence can still occur with supercooled droplets which then freeze on contact with the ground.

(c) *Dew*
Not common; it requires road surface temperature (RST) to fall below dew point and sufficient breeze to mix air in vicinity of road surface.

(d) *Hoar frost*
Not common; problems occur after traffic has traversed it, changing it to ice/water.

(e) *Freezing fog*
   (i) Although adjacent grass verges may be coated with rime, roads may be unaffected.
   (ii) As the fog thickens the ground temperature will rise as outgoing long-wave radiation is shut off.
   (iii) The RST may go above 0 °C even with a screen temperature as low as −1 °C.
   (iv) Widespread rime on roads is only expected if freezing fog is expected to remain shallow, or if the screen temperature is −1 °C or less.

(f) *Moisture advection over a cold surface*
   Particularly under increasing gradient with little cloud towards the end of a long radiation night. This process can also lead to ice formation after sunrise.

(g) *Melting snow*
   (i) Following snowfall the air temperature generally rises a little to give a slight daytime thaw and hence a source of moisture, leading to widespread icing after dark.
   (ii) Residual snow mounds left by snow ploughs can be very persistent and thus a potential source of road icing for days/weeks.

(h) *Seepage, springs, etc.*
Not strictly a meteorological problem, but can follow a prolonged period of winter rain, maintaining a verge or road wet even when conditions are dry.

Astbury (1994)
Hewson & Gait (1992)

2.6.2.1 Forecasting hoar frost

The following are necessary for hoar frost:
RST to be below air-mass dew point and to be at or near freezing; breeze sufficient to cause mixing.

These conditions are likely if five or more of the following conditions are satisfied:
(i) long night;
(ii) low road-depth temperature (RDT) ($\leq$4.5 °C);
(iii) clear sky $\leq$2/8 cloud cover;
(iv) wind $\geq$4 kn at 10 m;
(v) high dew point $\geq$1 °C;
(vi) small dew-point depression $\leq$1.5°C;
(vii) cold and clear previous night.

Adjacent moisture sources, such as small lakes, rivers, edges of woods, etc. are important.

Local variations: more likely to be encountered on higher ground, in coastal regions, on bridge decks.

Note that:
(i) Hoar frost is unlikely in very cold, dry air; early or late in the season.
(ii) The five conditions are most likely during polar maritime and arctic maritime outbreaks when the higher, colder more exposed sites become frosty first.
(iii) Most severe events occur when moister air with RDT higher than RST is being advected over a cold surface after a cold spell.
(iv) During several days of clear skies north facing slopes, sheltered urban and rural roads can accumulate hoar frost over several days and nights.

Thermal maps can aid the forecaster in constructing the likely spatial variability to be anticipated in road-surface temperatures under clear, cloudy, windy, wet, etc. nights.

Astbury (1994)
Hewson & Gait (1992)
Perry & Symons (1991)

2.7 Modification of surface air temperature over the sea

2.7.1 Advection of cold air over warm sea

2.7.1.1 Frost's method

If T_o (°C) and r_o (g kg^{-1}) are the temperature and humidity mixing ratio of the air before crossing the sea, T and r the values after crossing at least 60 miles of sea; T_s and r_s are the sea temperature and humidity mixing ratio of saturated air at temperature T_s, then:

$$T = T_o + 0.6\,(T_s - T_o)$$
$$r = r_o + 0.6\,(r_s - r_o).$$

Notes:
(a) These formulae apply to all cold airstreams crossing a warmer sea surface, e.g. a cold northerly outbreak reaching north Scotland or a cold westerly current reaching Norway.
(b) In applying these formulae, make the best estimate of the sea-surface temperature along the trajectory. Determine r_o and r_s by using a tephigram.
(c) Although this method is simple to use it has been criticized because:
(i) The factor of 0.6 only applies to sea crossings of over 300 n mile (550 km).

(ii) The presence of any inversion is ignored.
(iii) The values of r can exceed the saturated humidity mixing ratio at the temperature T_s.

Frost (1941)

Blackall put forward a more empirically based method to overcome these objections.

2.7.1.2 Blackall's method

This is an empirically based method which takes into account both the duration of the sea crossing and the depth of convection. The method uses the equation

$$T = T_s - (T_s - T_o) \exp(-12t/d)$$

where T_s = sea temperature (°C), t is the duration of the sea crossing (hours), d is the depth of convection in hectopascals, and T is the final and T_o the original air temperature.

The procedure is as follows:

(a) On a sounding in the air upwind of the sea crossing, draw in the MSL isobar and, if necessary, extend the ascent downwards to meet this isobar at the coastal temperature.
(b) Draw a dry adiabatic through the sea temperature T_s **(Fig. 2.11)**. The pressure at which this line meets the environment curve is subtracted from the surface pressure to give the depth of convection d in hectopascals.
(c) Establish the expected lapse rate; if the air already has a lapse rate implying convection through the layer d, the environment curve should not be changed. If a lapse rate needs to be forecast modify the environment curve as follows: draw a line through the layer d with an appropriate lapse (use **Table 2.14**) such that the environment curve encloses equal areas (A and B in **Fig. 2.11(b)**) on each side of the line. Where this line meets the surface isobar is T_o. This step represents complete mixing without the addition of heat.
(d) Determine the time t that the air will spend over the sea from the wind in the layer d and the fetch. Using gradient winds from the isobars and 850 hPa contours should be sufficiently accurate in most cases.
(e) From **Table 2.14** look up the value of $\exp(-12t/d)$ using the appropriate values of t (hours) and d (hectopascals). Then find T from the equation, above.
(f) From temperature T on the surface isobar, draw a line parallel to the environment curve produced in step (c); this is the predicted environment curve when the air finishes its crossing.
(g) A mean value of the sea temperature will often give good answers; however, if changes in T_s alter the value of d and thus $\exp(-12t/d)$ it will be necessary to proceed by steps. This will also be necessary when the sea passage is expected to take more than 24 hours.

Note:
The procedure above does not allow for fronts and other dynamic means of heating and cooling. The increase in surface humidity mixing ratio is taken to be

$$r - r_o = 0.18\,(T - T_o)$$

with the dew point remaining constant with height.

Blackall (1973)

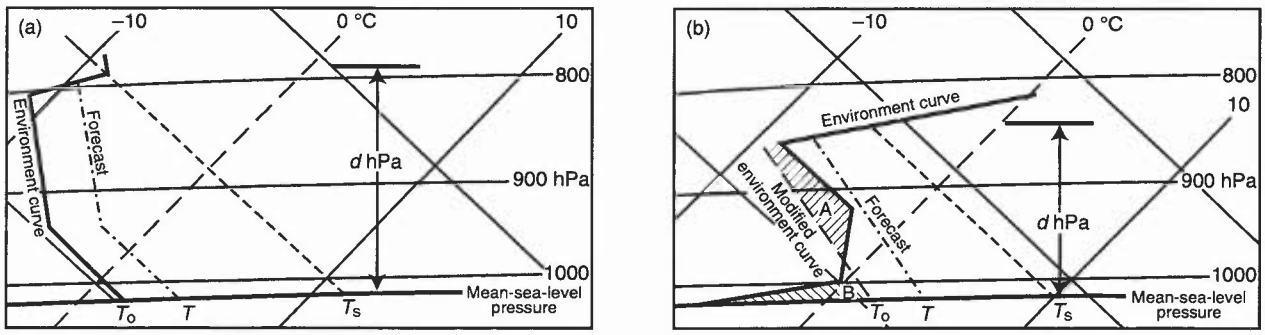

Figure 2.11. Forecasting the warming of cold air moving over a warm sea (Blackall's method) when (a) the upstream environment curve already indicates convective mixing is occurring, and (b) the environment curve is initially stable and needs modification. See text for details of construction.

Table 2.14. Values of exp (−12*t*/*d*).

Temp. lapse in the layer with depth *d* (°C)	*d* (hPa)	Duration of crossing *t* (hours)													
		1	2	3	4	5	6	7	8	9	12	15	18	21	24
	700	0.98	0.97	0.95	0.93	0.92	0.90	0.89	0.87	0.86	0.81	0.77	0.73	0.70	0.66
	600	0.98	0.96	0.94	0.92	0.90	0.89	0.87	0.85	0.84	0.79	0.74	0.70	0.66	0.62
40	500	0.98	0.95	0.93	0.91	0.89	0.86	0.84	0.82	0.81	0.75	0.70	0.65	0.60	0.56
31	400	0.97	0.94	0.91	0.89	0.86	0.84	0.81	0.79	0.76	0.70	0.64	0.58	0.53	0.49
26	350	0.97	0.93	0.90	0.87	0.84	0.81	0.79	0.76	0.73	0.64	0.60	0.54	0.49	0.44
22	300	0.96	0.92	0.89	0.85	0.82	0.79	0.76	0.73	0.70	0.62	0.55	0.49	0.43	0.38
17	250	0.95	0.91	0.86	0.83	0.79	0.75	0.71	0.68	0.65	0.57	0.49	0.42	0.36	0.32
14	200	0.94	0.89	0.84	0.79	0.74	0.70	0.66	0.62	0.58	0.49	0.41	0.34	0.28	0.24
13	180	0.94	0.88	0.82	0.77	0.72	0.67	0.63	0.59	0.55	0.45	0.37	0.30	0.25	0.20
12	160	0.93	0.86	0.80	0.74	0.69	0.64	0.59	0.55	0.51	0.41	0.33	0.26	0.21	0.17
10	140	0.92	0.84	0.77	0.71	0.65	0.60	0.55	0.50	0.46	0.36	0.28	0.21	0.17	0.13
9	120	0.90	0.82	0.74	0.67	0.61	0.55	0.50	0.45	0.41	0.30	0.22	0.17	0.12	0.09
8	100	0.89	0.79	0.70	0.62	0.55	0.49	0.43	0.38	0.34	0.24	0.17	0.12	0.08	0.06
6	80	0.86	0.74	0.64	0.55	0.47	0.41	0.35	0.30	0.26	0.17	0.11	0.07	0.04	0.03
5	60	0.82	0.67	0.55	0.45	0.37	0.30	0.25	0.20	0.17	0.09	0.05	0.03	0.01	
4	50	0.79	0.62	0.49	0.38	0.30	0.24	0.19	0.15	0.12	0.06	0.03	0.01		
4	40	0.74	0.55	0.41	0.30	0.22	0.17	0.12	0.09	0.07	0.03	0.01			
1	30	0.67	0.45	0.30	0.20	0.14	0.09	0.06	0.04	0.03	0.01				

2.7.1.3 Grant's method

(a) Use air trajectory and wind speed to find length of fetch(es).

(b) Use sea temperature charts to find the mean sea temperature (T_s) and from a tephigram, determine the saturated humidity mixing ratio (r_s) at this temperature.

(c) On a representative upstream sounding:
  (i) Draw in the MSL isobar (p_s).
  (ii) Draw a dry adiabat from T_s to meet the environment curve.
  (iii) Draw the isobar through this meeting point and note the depth of convection (d) in hectopascals.

(d) Modify the initial air temperature (T_o) by
  (i) Drawing the expected condensation level (CL) at end of sea crossing. Use $p_s - 60$ hPa as a first guess.
  (ii) If the sounding is well inland, modify the lower part to fit the reported temperatures at the upwind coast.
  (iii) Draw the path followed by a parcel of air condensing at the expected CL so that equal areas (A = B) are enclosed between the path curve, the environment curve and the isobar $p_s - d$ (**Fig. 2.12**).
  (iv) Note value of modified initial temperature (T_o).
  (v) Note value of $T_s - T_o$. This is used in (f)(ii) below.

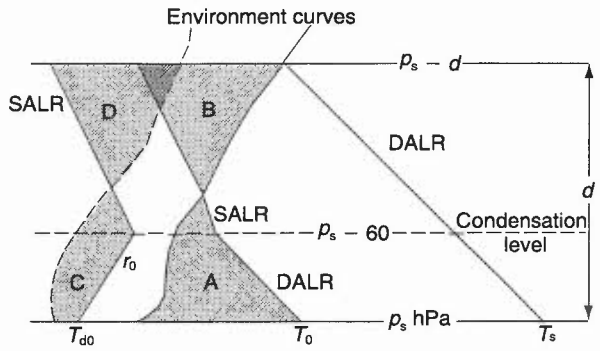

Figure 2.12. Forecasting the warming of cold air moving over a warm sea (Grant's method) — the modification of an initially stable temperature and moisture structure where T_s is the sea temperature at mean-sea-level pressure (p_s), ($p_s - 60$) is a first estimate of condensation level and ($p_s - d$) is the expected top of the convective layer. See text for method of construction.

(e) Modify the initial mixing ratio (r_o)
   (i) Draw a constant-mixing-ratio line up to the CL and a saturated adiabat above, so that the total water-vapour content between the isobars p_s and $p_s - d$ is unchanged. Since water content is not proportional to area this construction is not an 'equal area' one, but the lower area where water content is large must be less than the upper one where water contents are smaller, i.e. area C<area D.
   (ii) Note the modified value of r_o.

(f) Use the nomogram in **Fig. 2.13**.
   (i) Starting from the scale for 'fetch', move horizontally to 'd', the depth of convection, and from this point draw a line downward to the lower part of the nomogram.
   (ii) Enter left-hand scale for $(T_s - T_o)$ and draw a horizontal line to meet the vertical. The meeting point is marked by a small circle on the example plotted on **Fig. 2.13**
   (iii) Read off the value ΔT from the family of full curves. The downwind temperature is then $T_o + \Delta T$.
   (iv) Read off Z to the nearest 0.01 from the family of pecked curves.
   The final mixing ratio is given by

$$r = r_o + Z\,(r_s - r_o).$$

   (v) Use a tephigram to convert 'r' to the corresponding dew point T_d.
   (vi) The final CL is given approximately by 120 $(T - T_d)$ m
   or 400 $(T - T_d)$ ft.

This method of forecasting coastal temperatures in cold-air advection with onshore winds appears to perform better than Blackall's method, though giving no real improvement in showery northerlies.

Grant (1975)

2.7.2 Advection of warm air over a cold sea (Lamb and Frost's method)

For surface winds less than 20 kn

$$T - T_s = (T_s - T_o)\,\mathrm{f}(d)$$
$$r - r_s = (r_s - r_o)\,\mathrm{f}(d)$$

where d is the fetch (km) over the sea and other symbols are as in Frost's method.

Table 2.15. Values of f(d)

d (km)	100	200	300	400	500	600	700	800	900	1000
f(d)	0.175	0.152	0.141	0.133	0.127	0.123	0.119	0.116	0.113	0.110

Note: A cool sea surface exerts a powerful and rapid control on the temperature at screen height.

Lamb (1943)

2.8 Cooling of air by precipitation

2.8.1 Cooling of air by rain

A dry-bulb temperature close to the wet-bulb value is reached after about half an hour of very heavy rain or about 1 to 2 hours of rain of lesser intensity.

HWF (1975) Chapter 14.9.3

2.8.2 Cooling of air by snow

Falling snow gradually lowers the 0 °C level. However, the reduction of the surface temperature to 0 °C is unlikely if:
(i) the wet-bulb temperature at the surface is higher than 2.5 °C in prolonged frontal precipitation;
(ii) the wet-bulb temperature at the surface is higher than 3.5 °C within extensive areas of moderate or heavy instability precipitation.

Note: The relation between wet-bulb temperature and the form of precipitation is given in 5.10.1.

Lumb (1963)

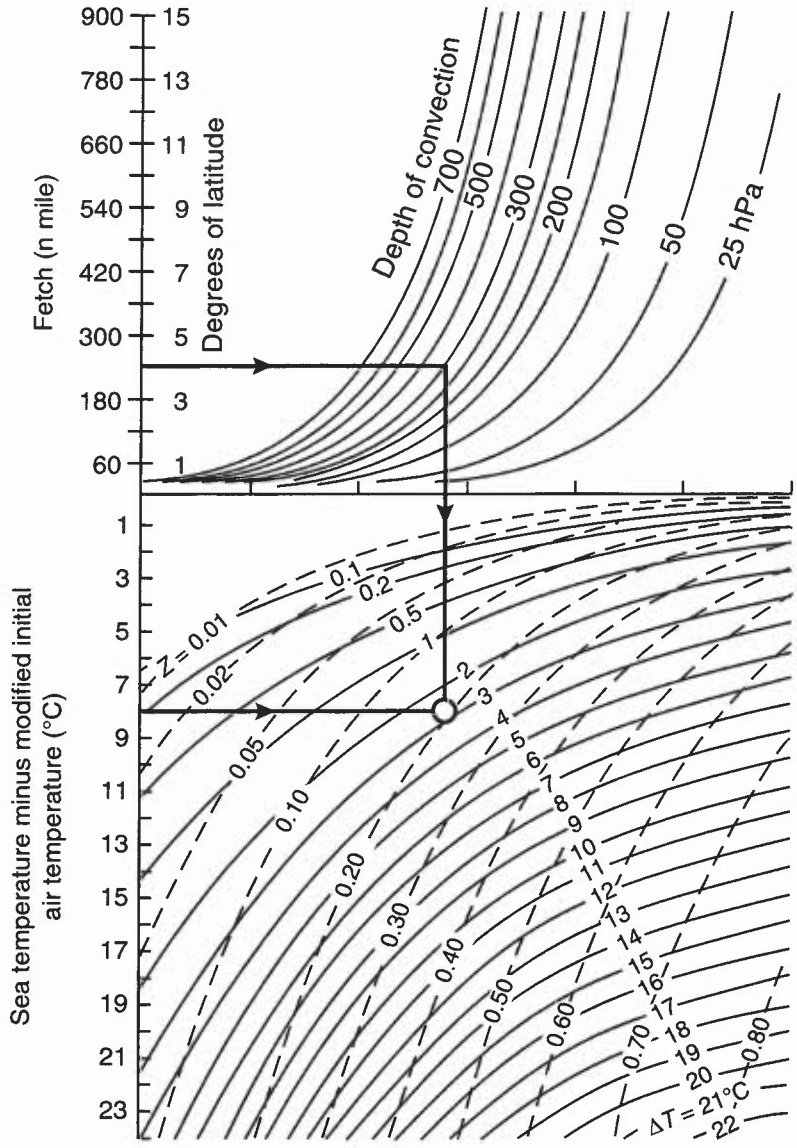

Figure 2.13. Nomogram for determining the surface temperature increase (ΔT) from the fetch(es), the depth of convection and the sea–air temperature difference. The pecked lines show isopleths of the moisture lines, Z. See text for method of use.

2.8.3 Downdraught temperatures in non-frontal thunderstorms

The temperatures of strong downdraughts reaching the ground are very close to the surface temperature of the saturated adiabatic through the intersection of the wet bulb and the 0 °C isotherm (6.2.2.4) **(Fig. 6.4)**.

Fawbush & Miller (1954)

2.9 Ice accretion

2.9.1 Types of icing

Table 2.16. Types of icing

Type	Source	Formation and properties
Hoar frost	Vapour	Direct deposition on surface with temperature below frost point of ambient air. White crystalline coating.
Rime	Supercooled droplets	Impact on surface with temperature <0 °C. Variable properties. Two extreme forms are: (a) *Opaque rime*: Drops freeze rapidly without much spreading; light porous texture with a lot of entrapped air; the smaller the droplets and the lower the temperature the rougher and more cloudy will be deposit. (b) *Clear, or glazed, ice*: Drops spread and freeze more slowly; smooth and glassy deposit sticks strongly to surface (temperatures near 0 °C).
Rain ice	Supercooled	Formation similar to clear ice. Substantial deposits may form over an extensive region. The resulting low-level icing may be severe; it is not common, but is a very important forecasting challenge in the UK and near continent (see 2.9.9).
Cloudy or mixed ice	Supercooled and ice	Ice crystals may adhere to wet surface and freeze in with droplets to give a rough, cloudy ice.
Pack snow	Supercooled drops and snowflakes	Drops freeze on impact, embedding the snowflakes, giving deposit like tightly packed snow.

HAM (1994)

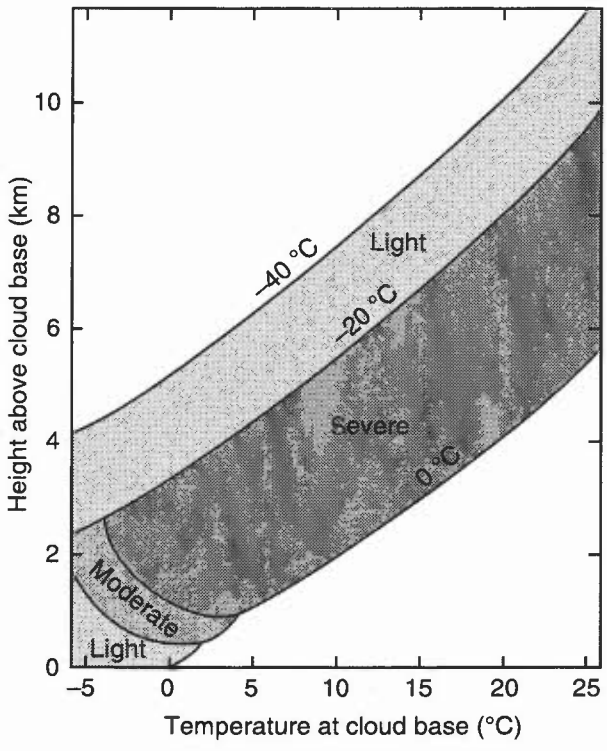

Figure 2.14. Airframe icing in convection cloud. Approximate thickness of layers within which various degrees of icing may be expected to occur. Base of cloud = 950 hPa, ambient relative humidity = 70%.

2.9.2 Airframe icing

Ice accretion on an airframe is possible whenever flight occurs through cloud or rain at sub-zero temperatures **(Fig. 2.14)**, and on a rapid move from regions of low temperature to warm, moist regions. Potentially dangerous effects are:

(i) ice may alter the wing profile, reducing the available lift;
(ii) engine intakes may be blocked, causing loss of power;
(iii) weight of ice may overload the aircraft;
(iv) forward facing windows may be made opaque.

Pike (1995)

2.9.2.1 Icing risks for helicopters

Additional risks for helicopters are:

(i) Ice on rotating blades is especially dangerous, as they are more heavily loaded than a fixed aircraft wing. Uneven ice accretion, compounding the centrifugal loads, may cause severe vibration.
(ii) Cyclic pitch controls may become jammed, causing loss of control.

For commercial operations, principally in the North Sea, forecasts of liquid-water content and temperature are made available from numerical models.

HAM (1994)

2.9.2.2 'Cold-soak' icing as a result of 'Hi-Lo' profile flying

(i) Fast descent of military aircraft after prolonged flight at high levels with sub-zero temperatures can result in 'cold-soak' icing in no-cloud conditions.
(ii) Although the effect is usually short-term until ambient warming is effected, it becomes more important when descent temperatures are around the 0 °C level.
(iii) Kinetic airframe heating (typically at least 10 °C for transport aircraft) will offset the effect.

HAM (1994)

2.9.3 Engine icing

Engine icing can occur at temperatures above zero and in clear air. Many oceanic flights are now undertaken by twin-engined jets whose engines rely on their own power for anti-icing; engine loss forces descent to regions of high potential icing where ice build-up on an inoperative engine could attain 30 cm (1 ft) in a North Atlantic diversion.

2.9.3.1 Piston engines

In addition to *impact icing* piston engines are subject to:

(a) *Fuel icing* — due to water in fuel freezing — not common,
(b) *Carburettor icing* —
  (i) There are several types of carburettor with very different icing characteristics.
  (ii) Pressure reduction through venturi effect can reduce air temperature within (particularly float-type) carburettors by as much as 30 °C.
  (iii) There is thus a potential hazard for some types of aircraft even when temperatures are $\gg 0$ °C and is likely to present a greater hazard on humid summer days than on cold winter days.
  (iv) The pilot should be alert to clues that might suggest high ambient humidity such as: poor visibility; wet ground; nearby extensive water surface; just below cloud base; in clear air just after fog dispersal.

CAA (1991)

2.9.3.2 Turbine and jet engines

(i) Susceptible parts are intake rim and struts; icing will be proportional to rate of airflow through engine.
(ii) Adiabatic expansion in the intake can cause temperature drop of up to 5 °C.
(iii) Prolonged flight near 0 °C in moist air might result in icing of engine while not occurring on the airframe.

2.9.4 Intensity of ice accretion

Terms used to describe ice accretion are: Trace of icing, light, moderate and severe icing.

(i) These terms can be used to *report* ice accretion but not for *forecasting* purposes since icing intensity is dependent on aircraft type and velocity vector.

(ii) The *depth* of the icing layer ('icing band') is always required by aircrew in order to plan for avoidance or rapid transit of the band.

HAM (1994)
WMO (1968)

2.9.5 Icing and liquid-water content

(i) The relationship between the intensity of icing in clouds and supercooled liquid water content (LWC) is not simple.

(ii) It depends on the integral of the LWC (or rather that fraction that consists of droplets large enough to accrete to the aircraft) along the aircraft trajectory. Thus Fig. 2.14 is only a guide.

(iii) Critical value of the integral is 7.5 g cm^{-3}.

(iv) Forecasters should, in principle, forecast LWC using model guidance and/or methods in 2.9.6 and 2.9.7.5, allowing the user to calculate integrals along aircraft trajectories (consistent methodology required of the user).

(v) Forecasters must be aware that the propensity for droplets to accumulate on an aircraft depends critically on both drop size and the size of the aircraft component; a large proportion of cloud drops are of sizes that are efficiently collected by small components (e.g. pitot-static tubes) on fast aircraft but are collected much less efficiently on large components on slow-moving aircraft.

2.9.6 Estimating the maximum liquid-water content of a cloud

On a tephigram:

(a) Plot the pressure and temperature at cloud base.

(b) Ascend along a saturated adiabat to the cloud-top level.

(c) The difference in HMR between the base and top of the cloud gives the maximum (adiabatic) liquid-water content of the cloud, in units of g kg^{-1}.

Since at 800 hPa (a typical wet-cloud level) 1 kg of air occupies about 1 m^3, the number obtained in (c) may simply be relabelled in units of g m^{-3}, which is a more useful measure of liquid water content for practical measurement.

Modifying factors

(i) Mixing with dry air at cloud top may reduce the actual cloud water content to around half the theoretical maximum value.

(ii) Maximum values are only approached in a tiny fraction of the cloud volume.

(iii) Upward motion of the cloudy air increases the water content and the risk of icing at any level.

(iv) Strong upcurrents in convective clouds produce the most severe icing, but orographic and frontal upslope motions may also produce severe ice accretion at times.

Note that orographic uplift can significantly lower the freezing level, giving icing at unexpectedly low levels. The importance of the increase in icing severity thus encountered cannot be overemphasized.

2.9.7 Cloud temperature and icing risk

2.9.7.1 Convective clouds

(i) Cloud-base temperature influences the risk and severity of ice accretion; the average liquid-water content/unit volume shows little variation with that over most of the cloud depth.

(ii) However, there is a higher liquid-water content in newly developing parts of a Cu cloud than in the more mature regions; liquid droplets predominate down to about −15 °C.

(iii) Large cloud-water mixing ratios can exist at high altitude. Incidents of severe icing have been reported in developing Cb anvils, the tropopause restricting vertical development, thereby producing an extensive layer of liquid and frozen water.

The following rules are generally accepted:

Table 2.17.

Cloud temperature (°C)	Nature of cloud particles: Supercooled water	Nature of cloud particles: Ice crystals	Icing risk
0 to −20	many	few	High
−20 to −40	few	many	Low (but High in Cb cells and see (iii) above))
<−40	nil	all	nil

Fig. 2.14 illustrates the potential for airframe icing in convective clouds under various cloud-base temperature conditions, but see 2.9.4 and 2.9.5.

Lunnon et al. (1994)

2.9.7.2 Layer cloud

Generally the icing severity in layer clouds of about 3000 ft thickness and tops at 850 hPa is:

(a) *moderate* for tops between 0 and −10 °C;
(b) *light* for tops <−10 °C.

Satellite imagery is useful in pinpointing the rapid build-up of cloud frequently responsible for icing.

It is important to note:

(i) The risk of icing increases above the lowest 300 m of the cloud.
(ii) Even in layer cloud, such as anticyclonic stratocumulus forming over the sea in winter, the icing in the upper part of the cloud may be severe. This is due both to the high liquid-water content and to duration of flight possible within extensive cloud layers. A capping inversion will further encourage the maintenance of a high liquid-water content by restricting the depth for drop growth by the Bergeron–Findeisen method.
(iii) Altocumulus and nimbostratus, formed by mass ascent, may be extensive and deep; icing will be further enhanced by orographic lifting. Severe icing has been reported at temperatures as low as −20 to −25 °C.

2.9.7.3 Cirrus

Cirrus clouds seldom constitute an icing hazard.

2.9.7.4 Orographic cloud

Icing is likely to be more severe in clouds subject to orographic lift than in similar clouds away from high ground.

2.9.7.5 Cloud type: summary table of icing probability and intensity

Liquid water content increases from zero at just below cloud base roughly linearly for the first 200–300 m above cloud base. In this region there is little or no icing, unless there is orographic uplift or embedded convective cloud.

Table 2.18.

Cloud type	Probability of icing	Intensity	Water content ($g\ m^{-3}$)
Cb, Ns	High	May be severe	0.2–4.0
Cu, Sc, Ac, AcAs	50%	Rarely more than moderate	0.1–0.5
As	Low	Moderate or light	0.1–0.3
St	Low	Light	0.1–0.5
Upper regions of layer cloud	High	May be severe	0.5–1
Orographic	High	probably moderate	0.1–0.5

Note that the severity is also a function of other non-meteorological factors: aircraft type and duration of flight within the cloud (2.9.4).

HAM (1994)

2.9.8 Freezing rain in elevated layers (see 5.9.7)

Ahmed et al. (1993)

2.9.9 Severe low-level icing (rain ice) (see 5.9.8)

HWF (1975), Chapter 19.7.8

2.9.10 Slantwise convection (conditional symmetric instability)

Generally θ_w surfaces are roughly parallel to the earth's surface while surfaces of constant momentum are vertical. Occasionally, however, θ_w surfaces can become more vertical than the momentum surfaces (e.g. in association with fronts), and air parcels can then move considerable distances up these θ_w surfaces (slantwise convection) without experiencing any restoring force. Severe icing events are often associated with this slantwise convection.

Bohorquez & McCann (1995)

2.9.11 Icing on ships

(i) In rough seas when the wind is strong and the air temperature below −2 °C, spray may freeze on the superstructure of a vessel. The weight of accumulated ice may eventually become a considerable hazard.

(ii) The degree of icing depends on both temperature and wind speed, as shown in **Fig. 2.15**. The icing is classified in terms of thickness of accumulation per day (**Table 2.19**).

Table 2.19.

Degree of icing	Accumulation (cm per 24 hours)
Light	1–3
Moderate	4–6
Severe	7–14
Very severe	15 or more

HWF (1975), Chapter 21.5.2

2.10 Wind chill and heat stress in man and animals

2.10.1 Human perception of wind chill

The influence of wind on the human perception of temperature gives rise to an 'equivalent temperature' (not applicable to inanimate objects). Steadman's data (**Table 2.20, Fig. 2.16**) relate to the still air temperature for which the rate of heat loss from a human is the same as that for the observed wind and temperature.

C & PSH, Chapter 3.10.3
Dixon & Prior (1987)
Steadman (1984)

2.10.2 Heat stress, mass participation events

Many heat stress indices have been devised. The Temperature–Humidity Index (THI) is applicable to sedentary workers indoors, or outside in the shade in light winds and can be forecast from the dry- and wet-bulb temperatures (T and T_w) as follows:

$$\text{THI} = 0.4(T + T_w) + 4.8 \text{ (in °C)}.$$

As THI increases above 20, increasing discomfort is felt; at THI = 24 some 50% of people are expected to feel discomfort; for THI >27 all are likely to be distressed.

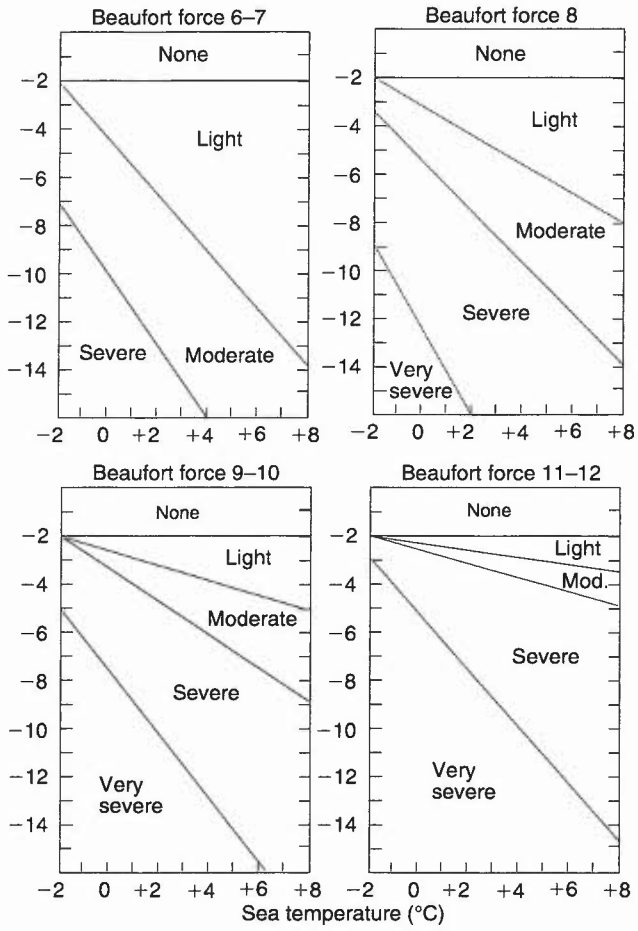

Figure 2.15. Icing on slow-moving fishing vessels in various wind conditions.

Table 2.20. Wind-chill equivalent temperatures (Steadman)

Screen temp. (°C)	10-metre wind (knots)							
	5	10	15	20	25	30	35	40
20	19.1	17.4	15.9	14.9	14.0	13.3	12.8	12.3
18	17.0	15.2	13.7	12.5	11.5	10.8	10.2	9.7
16	14.9	13.0	11.4	10.1	9.0	8.2	7.6	7.0
14	12.9	10.8	9.1	7.6	6.5	5.6	4.9	4.2
12	10.8	8.6	6.7	5.2	4.0	3.0	2.1	1.4
10	8.7	6.4	4.4	2.7	1.4	0.2	−0.6	−1.4
8	6.7	4.2	2.0	0.2	−1.2	−2.5	−3.4	−4.2
6	4.6	2.0	−0.4	−2.3	−3.9	−5.2	−6.3	−7.0
4	2.5	−0.3	−2.8	−4.8	−6.5	−7.9	−9.1	−10.0
2	0.4	−2.5	−5.2	−7.3	−9.1	−10.7	−11.9	−12.9
0	−1.7	−4.8	−7.5	−9.9	−11.8	−13.3	−14.6	−15.8
−2	−3.7	−7.1	−9.9	−12.3	−14.4	−16.1	−17.4	−18.6
−4	−5.8	−9.3	−12.3	−14.8	−17.0	−18.8	−20.2	−21.4
−6	−7.9	−11.6	−14.6	−17.3	−19.6	−21.3	−22.9	−24.2
−8	−10.0	−13.9	−17.0	−19.9	−22.2	−24.0	−25.6	−27.0
−10	−12.1	−16.1	−19.4	−22.4	−24.7	−26.6	−28.3	−29.5
−12	−14.2	−18.3	−21.7	−24.9	−27.3	−29.3	−31.0	−32.6
−14	−16.3	−20.6	−24.1	−27.3	−29.9	−31.9	−33.8	−35.3
−16	−18.3	−22.8	−26.5	−29.7	−32.4	−34.6	−36.5	−38.0
−18	−20.4	−25.0	−28.9	−32.2	−34.9	−37.2	−39.1	−40.8
−20	−22.5	−27.2	−31.2	−34.7	−37.4	−39.7	−41.7	−43.5

The potential for heat stress in mass participation 'fun-run' events is considerable and this must be pointed out in any forecasts specifically for such events; crowding restricts airflow and the ability of the body to dissipate the heat load imposed by high levels of temperature, humidity and solar radiation.

Driscoll (1985)
de Freitas et al. (1985)
Kerslake (1972)
Steadman (1984)

2.10.3 Wind chill and heat stress in livestock

Heat loss from lambs, particularly if wet, in the first few hours after birth can impose enormous stress which may result in death. Forecast advice is available to farmers. Housed livestock, including chickens, are liable to heat stress, particularly under crowded conditions; warnings to livestock managers are available when temperatures of >23 °C are expected for more than 3 hours.

C & PSH, Chapter 6
Starr (1988)

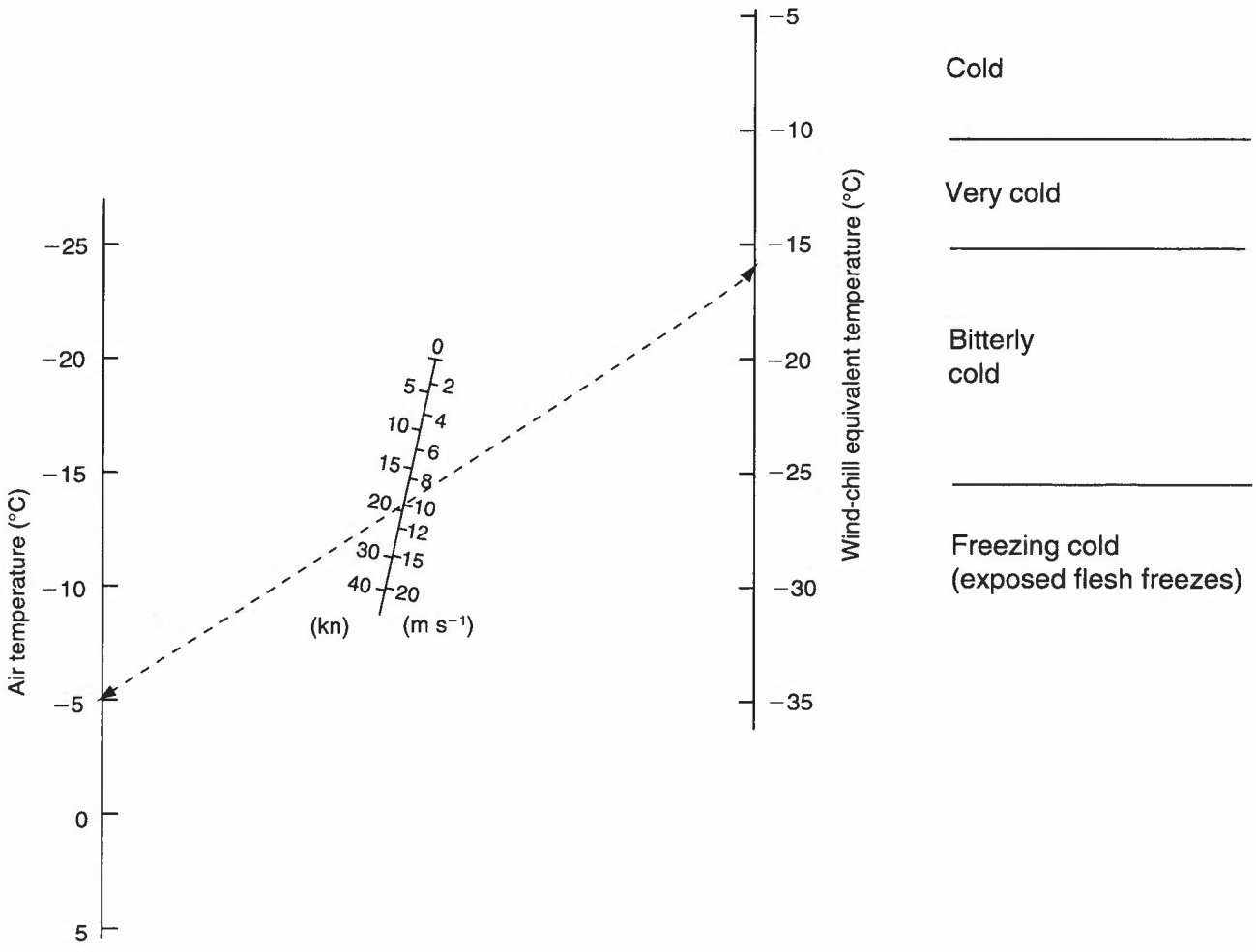

Figure 2.16. Nomogram for obtaining Steadman (1984) wind-chill equivalent temperatures and associated sensations for various combinations of air temperature and 10 m wind speed. The example shows an equivalent temperature of −16 °C, which would be termed 'bitterly cold', resulting from an air temperature of −5 °C and a wind speed of 20 kn.

2.11 The urban 'heat island'

The urban environment will influence heat storage and the radiation balance; the result is a modified local (micro-) climate compared with the surrounding rural environment:

(i) Rural areas typically form surface inversions under good nocturnal radiation conditions.
(ii) Over the city this 'heat island' maintains a shallow, convectively mixed, approximately isothermal, layer. Hence at about 50 m rural air may be warmer than city air (**Fig. 2.17**).
(iii) The layer is a function of population density, is less than 100 m deep and is most pronounced in the evening about 4 hours after sunset.
(iv) On a clear night over London temperature differences of more than 7 °C over the surrounding country have been measured.
(v) Under appropriate synoptic conditions this 'heat island' effect gives rise to thermal circulations and influences advection so as to, for example, induce severe storms.
(vi) Another effect is that the inner city may have its last frost several weeks earlier than the suburbs.
(vii) During the day the heat island effect is observable but, because of natural convection, is only 0.5 to 1 °C.
(ix) If a wind is present the 'heat island' might be eliminated; the breakdown depends on the size of the town. Limiting wind speeds are presented in **Table 2.21.**
(x) However, the presence of wind may cause excesses of temperature and deficits of humidity to be carried downwind with the urban pollution plume — which can be as wide as the city and transport for hundreds of kilometres. (1.3.4).
(xi) An implication is that visibility may be reduced in the plume core by a factor of two compared with conditions in the country well away from the plume (3.9.1).

Table 2.21. Limiting wind speed for development of heat islands

Population	Surface wind (kn)
10 million	25
2 million	22
500 thousand	16
250 thousand	12
100 thousand	10
50 thousand	9
25 thousand	8

Landsberg (1981)
Oke (1987)

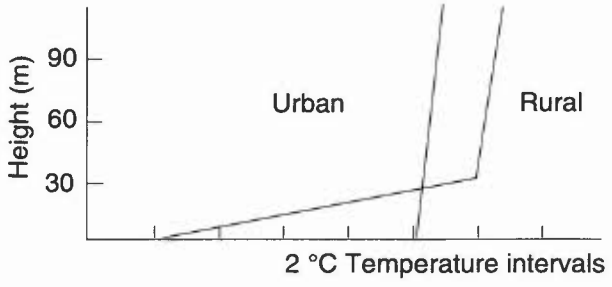

Figure 2.17. The difference of the urban heat-island on an urban and an adjacent rural temperature profile (see text).

2.12 Model Output Statistics (MOS)

(i) MOS models match observations and forecast parameters; a statistical relationship is established, the MOS technique thus allowing for bias in the model forecast by the post-processing of model data. Station-specific maximum and minimum temperatures are available.

(ii) Current parameters used in MOS regressions are:
MSLP (of little value);
level 1 (997 hPa): temperature, dew point, wind speed and direction;
level 4 (870 hPa): temperature, dew point, wind speed and direction;
vertical shear parameter (of minor significance).

(iii) MOS are not well equipped to forecast extreme temperatures.

(iv) MOS temperatures from the LAM are occasionally misleading due to poor representation of boundary layer cloud, particularly when Sc is trapped below an inversion lower than model level 4, with dry air above (giving too low minima).

(v) Changes in model formulation can affect maximum temperatures, giving a temporary deterioration in accuracy until the new model characteristics have been 'learnt' by the MOS model.

(vi) Forecasters must examine structure of low-level flow before using MOS values.

(vi) MOS forecasts are based on midday and midnight ascents for maximum and minimum temperature, respectively. Changes after these times, e.g. the passage of a cold front in the early hours of the morning, cannot be taken into account; beware situations when the base of an inversion is lower than 870 hPa (level 4).

(vii) MOS algorithms are updated monthly.

(viii) Around equinoxes rapid changes in insolation may lead to inaccurate forecasts, e.g. too cold at beginning of September, too warm at end of that month.

Glahn & Lowry (1972)
Ross (1989)

BIBLIOGRAPHY

CHAPTER 2 — TEMPERATURE

Ahmed, M., Graham, R.J. and Lunnon, R.W., 1993: Creating a global climatology of freezing rain using numerical model output. Proc. of Fifth Conference on Aviation Weather Systems, Am Meteorol Soc, Vienna (Virginia), USA.

Astbury, A., 1994: OpenRoad Manual, Meteorological Office (continuously updated).

Barthram, J.A., 1964: A method of forecasting a radiation night cooling curve. *Meteorol Mag*, **93**, 246–251.

Belasco, J.E., 1952: Characteristics of air masses over the British Isles. *Geophys Mem*, No. 87, London, Meteorological Office.

Blackall, R.M., 1973: Warming of the lower troposphere by the sea. *Meteorol Mag*, **102**, 65–73.

Bohorquez, M.A. and McCann, D.W., 1995: Model proximity soundings near significant aircraft icing reports. Proc. of Sixth Conf. on Aviation Weather Systems, Am Meteorol Soc, Dallas, Texas, USA.

Boyden, C.J., 1937, A method for predicting night minimum temperatures. *QJR Meteorol Soc,* **63**, 383–392.

CAA, 1991: Piston engine icing. Safety Sense Leaflet No. 14, Civil Aviation Authority.

Callen, N.S. and Prescott, P., 1982: Forecasting daily maximum surface temperatures from 1000–850 mb thickness lines and cloud cover. *Meteorol Mag*, **111**, 51–58

C&PSH: Commercial and Public Services Handbook, Met.O.868, Meteorological Office (continuously updated).

Craddock, J.M. and Pritchard, D.L., 1951: Forecasting the formation of radiation fog — a preliminary approach. *Meteorological Research Paper* No. 624. Meteorological Office (unpublished).

de Freitas, C.R., Dawson, N.J., Young, A.A. and Mackey, W.J., 1985: Microclimate and heat stress in runners in mass participation events. *J Clim Appl Meteorol*, **24**, 184–191.

Dixon, J.C. and Prior, M.J., 1987: Wind-chill indices: a review. *Meteorol Mag*, **116**, 1–16.

Driscoll, D.M., 1985: Human health. Handbook of Applied Meteorology, pp. 778–814. John Wiley & Sons.

Fawbush E.J. and Miller, R.C. 1954: A basis for forecasting peak wind gusts in non-frontal thunderstorms. *Bull Am Meteorol Soc*, **35**, 14–19.

Frost, R., 1941: The influence of the North Sea on winter temperatures and dew points. Meteorological Office (unpublished).

Glahn, H.R. and Lowry, D.A., 1972: The use of MOS in objective weather forecasting. *J Appl Meteorol*, **11,** 1203–1211.

Grant, K., Fog frequencies in the UK relative to time of sunrise. *Special Investigations Paper*, Meteorological Office, (unpublished).

Grant, K., 1975: The warming and moistening of cold air masses by the sea. *Meteorol Mag*, **104**, 1–9.

HAM. Handbook of Aviation Meteorology, 1994: London, HMSO.

Hewson, T.D. and Gait, N.J., 1992: Hoar-frost deposition on roads. *Meteorol Mag*, **121**, 1–21.

HWF. Handbook of Weather Forecasting, 1975: Met.O.875, Meteorological Office.

Inglis, G.A., 1970: Maximum temperatures on clear days. *Meteorol Mag*, **99**, 355–363.

Jefferson, G.J., 1950: Temperature rise on clear mornings. *Meteorol Mag*, **79**, 33–41.

Johnson, D.W., 1958: The estimation of maximum day temperatures from the tephigram. *Meteorol Mag*, **87**, 265–266.

Kensett, C.H., 1983: Forecasting night minimum temperatures — a revision of McKenzie's method for 90 stations in the UK. Forecasting Techniques Memorandum No. 21. Meteorological Office.

Kerslake, D. McK., 1972: The stress of hot environments. Cambridge University Press.

Lamb, H.H., 1943: Haars or North Sea fogs on the coast of Great Britain. Meteorological Office (unpublished).

Landsberg, H.E., 1981: The Urban Environment. Academic Press.

Local Weather Manual (S England), 1994: Meteorological Office (PSP) publication.

Lumb, F.E. 1963: Downward penetration of snow in relation to the intensity of precipitation. *Meteorol Mag*, **92**, 1–14.

Lunnon, R.W., Holpin, G.E. and Anderson, S., 1994: Study of the meteorological conditions pertaining to 25 January 1994 BAe ALF502 rollback incident. Meteorological Office Research Tech. Report No. 102.

McKenzie, F., 1944: A method of estimating night minimum temperatures. *SDTM* No. 68. Meteorological Office, London (unpublished).

Oke, T.R., 1987: Boundary layer climates (2nd edition). Methuen.

Parrey, G.E., 1969: Minimum road temperatures. *Meteorol Mag*, **98**, 286–290.

Perry, A.H. and Symons, L.J., 1991: Highway meteorology. E & F.N. Spon.

Pike, W.S., 1995: Extreme warm frontal icing on 25 February 1994 causes an aircraft accident near Uttoxeter. *Meteorol Appl*, **2**, 273–279.

Ritchie, W.G., 1969: Night minimum temperatures at or near various surfaces. *Meteorol Mag*, **98**, 297–304.

Ross, G.H., 1989: Model Output Statistics. An updatable scheme. Am Meteorol Soc. 11th Conference on Probability and Statistics in the Atmospheric Sciences, Monterey, Ca, USA.

Saunders, W.E., 1952, Some further aspects of night cooling under clear skies. *QJR Meteorol Soc,* **78**, 603–612.

Sills, A.G., 1969: An investigation into the depression of the grass minimum temperature below the air minimum at Cottesmore. *Meteorol Mag*, **98**, 348–351.

Starr, J.R., 1988: Weather, climate and animal performance. Geneva, World Meteorological Organization, Technical Note 190.

Steadman, R.G., 1984: A universal scale of apparent temperatures. *J Clim Appl Meteorol,* **23,** 1674–1687.

WMO, 1968: Ice formation on aircraft. Geneva. (Reprint of 1961 publication). World Meteorological Organization, Technical Note 139.